

Heavy-Light Semileptonic Decays in Staggered Chiral Perturbation Theory

C. Aubin

Physics Department, Columbia University, New York, NY 10027

C. Bernard

Department of Physics, Washington University, St. Louis, MO 63130

Abstract

We calculate the form factors for the semileptonic decays of heavy-light pseudoscalar mesons in partially quenched staggered chiral perturbation theory (SXPT), working to leading order in $1/m_Q$, where m_Q is the heavy quark mass. We take the light meson in the final state to be a pseudoscalar corresponding to the exact chiral symmetry of staggered quarks. The treatment assumes the validity of the standard prescription for representing the staggered “fourth root trick” within SXPT by insertions of factors of $1/4$ for each sea quark loop. Our calculation is based on an existing partially quenched continuum chiral perturbation theory calculation with degenerate sea quarks by Bećirević, Prelovsek and Zupan, which we generalize to the staggered (and non-degenerate) case. As a by-product, we obtain the continuum partially quenched results with non-degenerate sea quarks. We analyze the effects of non-leading chiral terms, and find a relation among the coefficients governing the analytic valence mass dependence at this order. Our results are useful in analyzing lattice computations of form factors $B \rightarrow \pi$ and $D \rightarrow K$ when the light quarks are simulated with the staggered action.

PACS numbers: 12.39.Fe, 12.39.Hg, 11.30.Rd, 12.38.Gc

I. INTRODUCTION

Extraction of the CKM matrix elements $|V_{ub}|$ and $|V_{cs}|$ from the experimentally measured semileptonic decay rates for $B \rightarrow \pi \ell \nu$ and $D \rightarrow K \ell \nu$ requires reliable theoretical calculations of the corresponding hadronic matrix elements. Recently, there has been significant progress in computing these matrix elements on the lattice, with good control of the systematic uncertainties [1, 2, 3, 4]. Since computation time increases as a high power of the inverse quark mass, the light (u, d) quark masses used in the simulations are heavier than in nature, and a chiral extrapolation is necessary to obtain physical results. To keep systematic errors small, the simulated u, d masses should be well into the chiral regime, giving pion masses ~ 300 MeV or lighter. Such masses in lattice calculations of leptonic and semileptonic heavy-light decays are accessible with staggered quarks [5, 6, 7, 8, 9, 10]. The trade-off for this benefit is the fact that staggered quarks do not fully remove the species doubling that occurs for lattice fermions; for every flavor of lattice quark, there are four “tastes,” which are related in the continuum by an $SU(4)$ symmetry (or an $SU(4)_L \times SU(4)_R$ symmetry in the massless case). The taste symmetry is broken at non-zero lattice spacing a by terms of order a^2 .

The breaking of taste symmetry on the lattice implies that one must take into account taste-violations in the chiral extrapolations, leading to a joint extrapolation in both the quark masses and the lattice spacing. Staggered chiral perturbation theory (SXPT) [11, 12, 13] allows us to make such extrapolations systematic. For quantities with heavy quarks, one must also incorporate Heavy Quark Effective Theory (HQET) [14, 15, 16, 17, 18] into SXPT. This has been done in Ref. [19], and then applied to leptonic heavy-light decays. Here, we extend the analysis of Ref. [19] to the semileptonic case.

In addition to the practical implications of taste symmetry violations for chiral extrapolations, the violations lead to a potentially more serious theoretical concern. Simulations such as Refs. [5, 6, 7, 8, 9, 10, 20] take the fourth root of the staggered quark determinant [21] in an attempt to obtain a single taste per quark flavor in the continuum limit. Were the taste symmetry exact at finite lattice spacing, the fourth root prescription would obviously accomplish the desired goal, since it would be equivalent to using a local Dirac operator obtained by projecting the staggered operator onto a single-taste subspace. Because the taste symmetry is broken, however, the fourth root is necessarily a nonlocal operation at non-zero lattice spacing [22]. The question of whether the rooted theory is in the correct

universality class therefore becomes nontrivial. Nevertheless, there are strong theoretical arguments [22, 23, 24, 25, 26] in the interacting theory, as well as free-theory and numerical evidence [27] that the fourth-root trick is valid, *i.e.*, that it produces QCD in the continuum limit.

The current paper does not actually need to assume that the rooting procedure itself is valid.¹ Instead, like previous SXPT calculations for the rooted theory [12, 13, 19, 28], it requires a narrower assumption: that the rooting can be represented at the chiral level by multiplying each sea quark loop by a factor of $1/4$. This can be accomplished by a quark flow analysis [29], or, more systematically, by use of the replica trick [30]. In Ref. [24], it was shown that the correctness of this representation of the fourth root in SXPT follows in turn from certain — in our opinion, rather plausible — assumptions. As such, we assume here that this representation is valid. Fitting lattice quantities to SXPT formulae (as in Refs. [10, 20]) provides an additional empirical test of the validity of this representation.

The main purpose of the current paper is to find SXPT expressions for the form factors of the semileptonic decay $B \rightarrow P\ell\nu$, where P is some light pseudoscalar meson, which we will refer to generically as a “pion.” We consider first the partially quenched case, and obtain the full QCD results afterward by taking the limit where valence masses equal the sea masses. The B is a heavy-light meson made up of a b heavy quark and a valence light quark spectator of flavor x ; we use the notation B_x when confusion as to the identity of the light spectator could arise. The P meson (more precisely P_{xy}) is composed of two light valence quarks, of flavor x and y . For simplicity we consider only the case where the outgoing pion is (flavor) charged; in other words $x \neq y$. The flavor structure of the weak current responsible for the decay is $\bar{y}\gamma_\mu b$.

In our calculation, we take the heavy quark mass m_Q to be large compared to Λ_{QCD} and work to leading order in the $1/m_Q$ expansion. Our analysis also applies when the heavy quark is a c (*i.e.*, to D mesons), but we use B to denote the heavy-light meson to stress the fact that only lowest order terms HQET are kept. For D mesons, of course, the higher order terms omitted here would be more important than for B mesons.

Discretization errors coming from the heavy quark are not included in the current calculations. We assume that such errors will be estimated independently, using HQET as the

¹ Of course, were the fourth root trick to prove invalid, the *motivation* for the current work would be lost.

effective-theory description of the lattice heavy quark [31]. It is expected that the errors from staggered quark taste-violations, which are considered here, are significantly more important at most currently accessible lattice spacings than the heavy-quark errors [4]. However, since taste-violations decrease rapidly² when the lattice spacing is reduced, this may change in the not too distant future. In any case, the precise quantification of the total discretization error will always require simulation at several lattice spacings.

An additional practical constraint on the current calculation is that am_Q must not be too large compared to unity. When $am_Q \gg 1$, the effects of the heavy quark doublers would need to be included in the chiral theory, and the analysis would become prohibitively complicated. A detailed discussion of this and other issues involved in incorporating heavy quarks into SXPT appears in Ref. [19].

The calculations of interest here have been performed in continuum partially quenched chiral perturbation theory (PQ χ PT) by Bećirević, Prelovsek and Zupan [33] for N_{sea} degenerate sea quarks. In this paper we show how one can generalize the PQ χ PT formulae to the corresponding SXPT formulae, thereby avoiding the necessity of recomputing all the diagrams from scratch.

Some results from the current work, as well as a brief discussion of how to generalize PQ χ PT to SXPT, appear in Ref. [34]. In addition, our results have already been used in chiral fits to lattice data in Refs. [8, 9]. A related calculation for the $B \rightarrow D^*$ and $B \rightarrow D$ semileptonic form factors has been presented by Laiho and Van de Water [28].

The outline of this paper is as follows: We first include a brief description of heavy-light SXPT in Sec. II. In Sec. III, we discuss the procedure for generalizing PQ χ PT to SXPT, using the heavy-light form factors as examples, although the procedure can be used for many other quantities in SXPT. Using this procedure and starting from Ref. [33], we write down, in Sec. IV, the one-loop SXPT results for the semileptonic form factors. The partially quenched staggered case with non-degenerate sea quarks, as well as its continuum limit, is presented in Sec. IV A. In that section, we also discuss a method for treating — in a way that appears to be practical for fitting lattice data — some spurious singularities which arise in the calculations. Section IV B considers full-QCD special cases of the results from

² Taste violations with improved staggered fermions go like $\alpha_S^2 a^2$. See Fig. 1 in Ref. [32] for a test of this relation.

Sec. IV A; while Sec. IV C discusses the analytic contributions to the form factors at this order. In Sec. V we add in the effects of a finite spatial lattice volume. Sec. VI presents our conclusions. We include three appendices: Appendix A gives expressions for the S χ PT propagators and vertices, as well as the corresponding continuum versions. Appendix B lists the integrals used in the form factor calculations; while Appendix C collects necessary wavefunction renormalization factors that were calculated in Refs. [13, 19].

II. HEAVY-LIGHT STAGGERED CHIRAL PERTURBATION THEORY

References [14, 15, 16, 17, 18] show how to incorporate heavy-light mesons into continuum χ PT; the extension to S χ PT appears in Ref. [19]. Here we review the key features needed for our calculations.

The heavy-light vector ($B_{\mu a}^*$) and pseudoscalar (B_a) mesons are combined in the field

$$H_a = \frac{1 + \not{v}}{2} [\gamma_\mu B_{\mu a}^* + i\gamma_5 B_a] \ , \quad (1)$$

which destroys a meson. Here v is the meson velocity, and a is the “flavor-taste” index of the light quark in the meson. For n flavors of light quarks, a can take on $4n$ values. Later, we will write a as separate flavor (x) and taste (α) indices, $a \rightarrow (x, \alpha)$, and ultimately drop the taste index, since the quantities we calculate will have trivial dependence on the light quark taste. The conjugate field \overline{H}_a creates mesons:

$$\overline{H}_a \equiv \gamma_0 H_a^\dagger \gamma_0 = [\gamma_\mu B_{\mu a}^{\dagger*} + i\gamma_5 B_a^\dagger] \frac{1 + \not{v}}{2} \ . \quad (2)$$

As mentioned in the introduction, we use B to denote generic heavy-light mesons to emphasize that we are working to leading order in $1/m_Q$.

Under $SU(2)$ heavy-quark spin symmetry, the heavy-light field transforms as

$$\begin{aligned} H &\rightarrow SH \ , \\ \overline{H} &\rightarrow \overline{H}S^\dagger \ , \end{aligned} \quad (3)$$

with $S \in SU(2)$, while under the $SU(4n)_L \times SU(4n)_R$ chiral symmetry,

$$\begin{aligned} H &\rightarrow H\mathbb{U}^\dagger \ , \\ \overline{H} &\rightarrow \mathbb{U}\overline{H} \ , \end{aligned} \quad (4)$$

with $\mathbb{U} \in SU(4n)$ defined below. We keep the flavor and taste indices implicit here.

The light mesons are combined in a Hermitian field $\Phi(x)$. For n staggered flavors, Φ is a $4n \times 4n$ matrix given by:

$$\Phi = \begin{pmatrix} U & \pi^+ & K^+ & \cdots \\ \pi^- & D & K^0 & \cdots \\ K^- & \bar{K}^0 & S & \cdots \\ \vdots & \vdots & \vdots & \ddots \end{pmatrix}. \quad (5)$$

We show the $n = 3$ portion of Φ explicitly. Each entry in Eq. (5) is a 4×4 matrix, written in terms of the 16 Hermitian taste generators T_{Ξ} as, for example, $U = \sum_{\Xi=1}^{16} U_{\Xi} T_{\Xi}$. The component fields of the flavor-neutral elements (U_{Ξ} , D_{Ξ} , ...) are real; the other (flavor-charged) fields (π_{Ξ}^+ , K_{Ξ}^0 , ...) are complex. The T_{Ξ} are

$$T_{\Xi} = \{\xi_5, i\xi_{\mu 5}, i\xi_{\mu\nu}(\mu < \nu), \xi_{\mu}, \xi_I\}, \quad (6)$$

with ξ_{μ} the taste matrices corresponding to the Dirac gamma matrices, and $\xi_I \equiv I$ the 4×4 identity matrix. We define $\xi_{\mu 5} \equiv \xi_{\mu} \xi_5$, and $\xi_{\mu\nu} \equiv (1/2)[\xi_{\mu}, \xi_{\nu}]$.

The mass matrix is the $4n \times 4n$ matrix

$$\mathcal{M} = \begin{pmatrix} m_u I & 0 & 0 & \cdots \\ 0 & m_d I & 0 & \cdots \\ 0 & 0 & m_s I & \cdots \\ \vdots & \vdots & \vdots & \ddots \end{pmatrix}, \quad (7)$$

where the portion shown is again for the $n = 3$ case.

From Φ one constructs the unitary chiral field $\Sigma = \exp[i\Phi/f]$, with f the tree-level pion decay constant. In our normalization, $f \sim f_{\pi} \cong 131$ MeV. Terms involving the heavy-lights are conveniently written using $\sigma \equiv \sqrt{\Sigma} = \exp[i\Phi/2f]$. These fields transform trivially under the $SU(2)$ spin symmetry, while under $SU(4n)_L \times SU(4n)_R$ we have

$$\Sigma \rightarrow L \Sigma R^{\dagger}, \quad \Sigma^{\dagger} \rightarrow R \Sigma^{\dagger} L^{\dagger}, \quad (8)$$

$$\sigma \rightarrow L \sigma \mathbb{U}^{\dagger} = \mathbb{U} \sigma R^{\dagger}, \quad \sigma^{\dagger} \rightarrow R \sigma^{\dagger} \mathbb{U} = \mathbb{U} \sigma^{\dagger} L^{\dagger}, \quad (9)$$

with global transformations $L \in SU(4n)_L$ and $R \in SU(4n)_R$. The transformation \mathbb{U} , defined by Eq. (9), is a function of Φ and therefore of the coordinates.

It is convenient to define objects involving the σ field that transform only with \mathbb{U} and \mathbb{U}^\dagger . The two possibilities with a single derivative are

$$\mathbb{V}_\mu = \frac{i}{2} [\sigma^\dagger \partial_\mu \sigma + \sigma \partial_\mu \sigma^\dagger] , \quad (10)$$

$$\mathbb{A}_\mu = \frac{i}{2} [\sigma^\dagger \partial_\mu \sigma - \sigma \partial_\mu \sigma^\dagger] . \quad (11)$$

\mathbb{V}_μ transforms like a vector field under the $SU(4n)_L \times SU(4n)_R$ chiral symmetry and, when combined with the derivative, can form a covariant derivative acting on the heavy-light field or its conjugate:

$$\begin{aligned} (H \overleftarrow{D}_\mu)_a &= H_b \overleftarrow{D}_\mu^{ba} \equiv \partial_\mu H_a + i H_b \mathbb{V}_\mu^{ba} , \\ (\overrightarrow{D}_\mu \overline{H})_a &= \overrightarrow{D}_\mu^{ab} \overline{H}_b \equiv \partial_\mu \overline{H}_a - i \mathbb{V}_\mu^{ab} \overline{H}_b , \end{aligned} \quad (12)$$

with implicit sums over repeated indices. The covariant derivatives and \mathbb{A}_μ transform under the chiral symmetry as

$$\begin{aligned} H \overleftarrow{D}_\mu &\rightarrow (H \overleftarrow{D}_\mu) \mathbb{U}^\dagger , \\ \overrightarrow{D}_\mu \overline{H} &\rightarrow \mathbb{U} (\overrightarrow{D}_\mu \overline{H}) , \\ \mathbb{A}_\mu &\rightarrow \mathbb{U} \mathbb{A}_\mu \mathbb{U}^\dagger . \end{aligned} \quad (13)$$

The combined symmetry group of the theory includes Euclidean rotations (or Lorentz symmetry), translations, heavy-quark spin, flavor-taste chiral symmetries, and the discrete symmetries C , P , and T . Many of these symmetries are violated by lattice artifacts and/or light quark masses. Violations to a given order are encoded as spurions in the Symanzik action. From these spurions, the heavy-light and light-light fields, derivatives, the heavy quark 4-velocity v_μ , and the light quark gamma matrix γ_μ , we can construct the chiral Lagrangian and relevant currents order by order.

Reference [19] finds the lowest order heavy-chiral Lagrangian and left-handed current, as well as higher order corrections. We need primarily the lowest order results here. For convenience, we write the Lagrangian in Minkowski space, so that we can make contact with the continuum literature.

We write the leading order (LO) chiral Lagrangian as

$$\mathcal{L}_{LO} = \mathcal{L}_{\text{pion}} + \mathcal{L}_{\text{HL}} \quad (14)$$

where $\mathcal{L}_{\text{pion}}$ is the standard SXPT Lagrangian [13] for the light-light mesons, and \mathcal{L}_{HL} is the contribution of the heavy-lights. We have³

$$\begin{aligned} \mathcal{L}_{\text{pion}} = & \frac{f^2}{8} \text{Tr}(\partial_\mu \Sigma \partial^\mu \Sigma^\dagger) + \frac{1}{4} \mu f^2 \text{Tr}(\mathcal{M} \Sigma + \mathcal{M} \Sigma^\dagger) \\ & - \frac{2m_0^2}{3} (U_I + D_I + S_I + \dots)^2 - a^2 \mathcal{V} , \end{aligned} \quad (15)$$

$$\begin{aligned} -\mathcal{V} = & C_1 \text{Tr}(\xi_5^{(n)} \Sigma \xi_5^{(n)} \Sigma^\dagger) + C_3 \frac{1}{2} \sum_\nu [\text{Tr}(\xi_\nu^{(n)} \Sigma \xi_\nu^{(n)} \Sigma) + h.c.] \\ & + C_4 \frac{1}{2} \sum_\nu [\text{Tr}(\xi_{\nu 5}^{(n)} \Sigma \xi_{5\nu}^{(n)} \Sigma) + h.c.] + C_6 \sum_{\mu < \nu} \text{Tr}(\xi_{\mu\nu}^{(n)} \Sigma \xi_{\nu\mu}^{(n)} \Sigma^\dagger) \\ & + C_{2V} \frac{1}{4} \sum_\nu [\text{Tr}(\xi_\nu^{(n)} \Sigma) \text{Tr}(\xi_\nu^{(n)} \Sigma) + h.c.] + C_{2A} \frac{1}{4} \sum_\nu [\text{Tr}(\xi_{\nu 5}^{(n)} \Sigma) \text{Tr}(\xi_{5\nu}^{(n)} \Sigma) + h.c.] \\ & + C_{5V} \frac{1}{2} \sum_\nu \text{Tr}(\xi_\nu^{(n)} \Sigma) \text{Tr}(\xi_\nu^{(n)} \Sigma^\dagger) + C_{5A} \frac{1}{2} \sum_\nu \text{Tr}(\xi_{\nu 5}^{(n)} \Sigma) \text{Tr}(\xi_{5\nu}^{(n)} \Sigma^\dagger) , \end{aligned} \quad (16)$$

$$\mathcal{L}_{\text{HL}} = -i \text{Tr}(\overline{H} H v \cdot \overleftarrow{D}) + g_\pi \text{Tr}(\overline{H} H \gamma^\mu \gamma_5 \mathbb{A}_\mu) . \quad (17)$$

Here Tr denotes a trace over flavor-taste indices and, where relevant, Dirac indices. The product $\overline{H} H$ is treated as a matrix in flavor-taste space: $(\overline{H} H)_{ab} \equiv \overline{H}_a H_b$. The covariant derivative \overleftarrow{D} acts only on the field immediately preceding it. For convenience, we work with diagonal fields (U, D, \dots) and leave the anomaly (m_0^2) term explicit in Eq. (15). We can take $m_0^2 \rightarrow \infty$ and go to the physical basis (π^0, η, \dots) at the end of the calculation [37].

To calculate semileptonic form factors, we need the chiral representative of the left-handed current which destroys a heavy-light meson of flavor-taste b . At LO this takes the form

$$j_{\text{LO}}^{\mu,b} = \frac{\kappa}{2} \text{tr}_D(\gamma^\mu (1 - \gamma_5) H) \sigma^\dagger \lambda^{(b)} , \quad (18)$$

where $\lambda^{(b)}$ is a constant vector that fixes the flavor-taste: $(\lambda^{(b)})_c = \delta_{bc}$, and tr_D is a trace on Dirac indices only.

The power counting is a little complicated in the heavy-light case, since many scales are available. Let m_q be a generic light quark mass, and let $m_\pi^2 \propto m_q$ be the corresponding “pion” mass, with p its 4-momentum. Further, take k as the heavy-light meson’s residual momentum. Then our power counting assumes $k^2 \sim p^2 \sim m_\pi^2 \sim m_q \sim a^2$, where appropriate powers of the chiral scale or Λ_{QCD} are implicit. The leading heavy-light chiral Lagrangian

³ There is a missing minus sign in Eq. (35) of Ref. [19].

\mathcal{L}_{HL} is $\mathcal{O}(k)$, the leading light-light Lagrangian $\mathcal{L}_{\text{pion}}$ is $\mathcal{O}(p^2, m_q, a^2)$, and the leading heavy-light current $j_{\text{LO}}^{\mu,b}$ is $\mathcal{O}(1)$. Only these leading terms are relevant to the calculation of non-analytic “chiral logarithms” at first non-trivial order, which give $\mathcal{O}(m_q, a^2)$ corrections to leading expressions for semileptonic form factors.

In principle, finding the corresponding analytic corrections requires complete knowledge of the next-order terms in the Lagrangian and current. However, since the form factors depend only on the valence and sea quark masses, a^2 , and the pion energy in the rest frame of the B (namely $v \cdot p$), the form of these corrections is rather simple and is easily determined by the symmetries. The large number of chiral parameters that can appear in higher-order terms in the Lagrangian and the current collapse down into relatively few free parameters in the form factors. Unless one wants to write these free parameters in terms of the chiral parameters, complete knowledge of the higher-order terms in the Lagrangian and current is often unnecessary. However, one does need to know enough about the higher-order terms to check for the possibility of relations among the free parameters that multiply different quantities or that appear in different form factors. At the order we work here, there is one relation among the various parameters that determine the linear dependence of the two form factors on the valence masses. In order to be sure that this relation is valid, we need to know all terms at next order that can contribute such linear dependence.

Fortunately, all such terms are known. For the light-light Lagrangian, Eq. (15), the relevant terms are the standard $\mathcal{O}(p^4 \sim m_q^2)$ terms in the continuum [38]. All terms of $\mathcal{O}(m_q a^2, a^4)$, which are special to S χ PT, are also available [39]. For the heavy-light Lagrangian and current, Ref. [19] lists all terms which are higher order than Eqs. (17) and (18) by a factor of m_q (most important here) or a^2 . Reference [19] does not attempt a complete catalog of the terms which are higher than Eqs. (17) and (18) by one or two powers of k , *i.e.*, having one or two derivative insertions. However, a sufficient number of representative terms of this type are listed to see that the corresponding free parameters in the form factors are all independent. We discuss the determination of the analytic terms further in Sec. IV C.

III. GENERALIZING CONTINUUM PQ χ PT TO S χ PT

We wish to compute the decay $B_x \rightarrow P_{xy}$ in S χ PT, where x and y are (light) flavor labels. The taste of the light quarks in B , P and the current also needs to be specified.

We take the P_{xy} to be a “Goldstone pion” with taste ξ_5 . Let the light quark in the B have taste α ($\alpha = 1, \dots, 4$); in flavor-taste notation the light quark has index $a \leftrightarrow x\alpha$. The current, Eq. (18), has flavor-taste $b \leftrightarrow y\beta$. Despite the existence of taste violations at non-zero lattice spacing, the amplitude turns out to be proportional to $(\xi_5/2)_{\alpha\beta}$, with a proportionality factor that is independent of the tastes α, β . We will often keep this rather trivial taste-dependence implicit.

In Ref. [33], Bećirević, *et al.* have calculated the form factors for $B \rightarrow \pi$ and $B \rightarrow K$ transitions in continuum PQχPT. They assume degenerate sea-quark masses, but leave N_{sea} , the number of sea quarks, arbitrary. As we explain below, the N_{sea} dependence is a marker for the underlying quark flow [29] within the meson diagrams. Once we have separated the meson diagrams into their contributions from various the quark flow diagrams, we can easily generalize the continuum PQχPT results to the staggered case, without actually having to calculate any SXPT diagrams. To check our method, however, we have also computed many of the diagrams directly in SXPT; the results agree.

The key feature that makes possible the generalization of continuum PQχPT results to SXPT results is the taste-invariance of the leading-order Lagrangian for the heavy-light mesons [19]. This means that the continuum vertices and propagators involving heavy-light mesons are trivially generalized to the staggered case: flavor indices (which can take N_{sea} values if they describe sea quarks) simply become flavor-taste indices (taking $4N_{\text{sea}}$ sea-quark values). In one-loop diagrams, taste violations arise only from the light meson (“pion”) propagators. Propagators and vertices for the staggered and continuum cases are listed Appendix A.

Looking at the expressions in Appendix B of Ref. [33], we see that there are two types of terms that can contribute to each diagram for $B_x \rightarrow P_{xy}$: a term proportional to N_{sea} , and a term proportional to $1/N_{\text{sea}}$. This is the same behavior that appears, for example, in light-light [35] or heavy-light [36] PQχPT decay constants.

The term which is proportional to N_{sea} comes solely from connected quark-level diagrams, an example of which is shown in Fig. 1 (where (a) is the meson-level diagram and (b) is the quark-level diagram).⁴ The appearance of the quark loop accounts for the factor of

⁴ By definition, the pion propagator in Fig. 1(a) is connected; the version with a disconnected propagator is shown in Fig. 2(a).

N_{sea} . In detail, using Eqs. (A15) and (A16), the loop integrand is proportional to the connected contraction $\sum_j \{\Phi_{ij}\Phi_{ji'}\}_{\text{conn}}$, where the index j is repeated because the heavy-light propagator conserves flavor. Equation (A18) then implies that the sum over j produces a factor of N_{sea} when the sea quarks are degenerate. In the non-degenerate case, there is no factor of N_{sea} but simply a sum over the sea-quark flavor of the virtual valence-sea pion.

In the staggered case, the internal heavy propagators, Eqs. (A1) and (A2), as well as the vertices coupling heavy-light mesons to pions (*e.g.*, Eq. (A3)), preserve both flavor and taste. Therefore Fig. 1 is now simply proportional to $\sum_b \{\Phi_{ab}\Phi_{ba'}\}_{\text{conn}} = \sum_{j\beta} \{\Phi_{i\alpha,j\beta}\Phi_{j\beta,i'\alpha'}\}_{\text{conn}}$, where we have replaced the flavor-taste indices (a, b, \dots) with separate flavor (i, j, \dots) and taste (α, β, \dots) indices. From Eq. (A8), the loop integrand is then proportional to

$$\sum_{j,\Xi} \frac{i\delta_{ii'}\delta_{\alpha\alpha'}}{p^2 - m_{ij,\Xi}^2 + i\epsilon} , \quad (19)$$

where the $\delta_{\alpha\alpha'}$ factor shows that, despite the existence of taste violations, the loop preserves the taste of the light quark in the heavy-light meson and is independent of that taste.

The overall factor of the SXPT diagram must be such as to reproduce the continuum result in the $a \rightarrow 0$ limit. Since pions come in 16 tastes, the sum over pion tastes Ξ in Eq. (19) must come with a factor of $1/16$ compared to the continuum expression. To see this explicitly, note first that there are two factors of $1/2$ relative to the continuum coming from the vertices (compare Eqs. (A3) and (A16)), due to the non-standard normalization of the taste generators, Eq. (6). An additional factor of $1/4$ comes from the SXPT procedure for taking into account the fourth root of the staggered determinant: This is a diagram with a single sea quark loop.

Finally, we need to consider how such a diagram depends on the tastes α and β of the heavy-light meson and the current. Since the taste indices flow trivially through the heavy-light lines and vertices, and, as we have seen, through the loops, the taste dependence is simply $(\xi_5/2)_{\alpha\beta}$, where the ξ_5 comes from the outgoing light meson. The factor of $1/2$ is due to the normalization of the taste generators.

The net result is that terms with factors of N_{sea} in the continuum calculation of Ref. [33] are converted to SXPT by the rule:

$$N_{\text{sea}}\mathcal{F}(m_M^2) \rightarrow \frac{(\xi_5)_{\alpha\beta}}{2} \frac{1}{16} \sum_{f,\Xi} \mathcal{F}(m_{fz,\Xi}^2) \quad (20)$$

where the sum over f is over the sea quark flavors, z is the valence flavor flowing through the loop (either x or y), m_M is the common mass of the N_{sea} mesons made up of a z valence quark and the degenerate sea quarks, and \mathcal{F} is some function of the pion masses. (For heavy-light quantities, \mathcal{F} is often also a function of the pion energy in the heavy-light rest frame.) The masses of pions of various tastes and flavors ($m_{fz,\Xi}$) are given in Eq. (A7).

The terms that are proportional to $1/N_{\text{sea}}$ are more subtle. They arise from diagrams with disconnected pion propagators. The simplest example is shown at the meson level in Fig. 2(a) and at the quark level in Fig. 2(b). The continuum form of the disconnected propagator is given in Eq. (A21). Using the continuum values $\delta' = m_0^2/3$ and $m_\eta'^2 \approx N_{\text{sea}} m_0^2/3$, we see that the disconnected propagator produces an overall factor of $1/N_{\text{sea}}$ as $m_0 \rightarrow \infty$. Equation (A21) can then be written as a sum of residues times poles, where the residues can be rather complicated when the sea masses are non-degenerate (see Appendix B). Thus, the final answer after integration amounts to something of the form

$$\frac{1}{N_{\text{sea}}} \sum_j \hat{R}_j \tilde{\mathcal{F}}(m_j^2) , \quad (21)$$

where $\tilde{\mathcal{F}}$ is again a general function resulting from the loop integral, \hat{R}_j is the residue of the pole at $q^2 = m_j^2$, and j ranges over the flavor-neutral mesons involved: the sea mesons, π_0, η, \dots , and the “external” mesons in the disconnected propagator, called ii and $i'i'$ in Eq. (A21). When $m_{i'i'} = m_{ii}$, there is a double pole, and Eq. (21) should be replaced by

$$\frac{1}{N_{\text{sea}}} \sum_j \frac{\partial}{\partial m_{ii}^2} \left[\hat{R}_j \tilde{\mathcal{F}}(m_j^2) \right] , \quad (22)$$

where the sum over j now does not include $i'i'$.

When the sea quarks are degenerate, the residues simplify considerably. However, by comparing the general forms in Eqs. (21) and (22) to the rather simple terms in Ref. [33], it is easy to move *backwards* from the degenerate case and determine the form of the expressions for non-degenerate sea quarks.

The flavor structure in the staggered case is identical to that in the continuum: Flavor remains a good quantum number, so meson propagators in both cases can only be disconnected if they are flavor neutral. Because of taste violations, however, disconnected hairpin diagrams can contribute to mesons propagators with three different tastes (singlet, vector, and axial vector) at this order in SXPT. These three hairpin contributions are quite similar to each other, but there are a few important differences:

- The strength of the hairpin, δ'_Ξ , depends on the taste Ξ — see Eq. (A9).
- In the taste-singlet case, as in the continuum, the hairpin ($4m_0^2/3$) comes from the anomaly and makes the flavor-singlet meson heavy. Decoupling the η'_I by taking $m_0^2 \rightarrow \infty$ is therefore a good approximation, and we do it throughout, giving rise to an overall factor of $1/N_{\text{sea}}$. But in the taste-vector and taste-axial-vector cases, the hairpins are not particularly large; indeed they are taste-violating effects that vanish like a^2 (up to logarithms) as $a \rightarrow 0$. So we cannot decouple the corresponding mesons, η'_V and η'_A , in the taste-vector and taste-axial-vector channels.
- The taste matrices associated with the vector and axial-vector mesons, ξ_μ and $\xi_{\mu 5}$, anticommute with the ξ_5 coming from the outgoing Goldstone pion. Therefore the vector and axial hairpin contributions will have an opposite sign from the singlet (and continuum) contribution if the ξ_5 needs to be pushed past a ξ_μ or $\xi_{\mu 5}$ to contract with the external pion state.

Figure 3 shows the tree-level diagrams that contribute to the form factors, while Figs. 4 and 5 show all the non-vanishing one-loop diagrams. As a first example of the treatment of diagrams with disconnected meson propagators, consider Fig. 5(b). It is not hard to see that this diagram has only a disconnected contribution, shown as a quark-flow diagram in Fig. 6. A connected contribution would require the contraction of the external light quark fields x and y , which make up the outgoing pion. That is impossible since we have chosen $x \neq y$.⁵

In our notation, the result from Ref. [33] for this diagram in the continuum partially quenched case with N_{sea} degenerate sea quarks is:

$$- \frac{g_\pi^2}{(4\pi f)^2} \frac{1}{N_{\text{sea}}} \left[\frac{m_Y^2 - m_U^2}{m_Y^2 - m_X^2} J_1^{\text{sub}}(m_Y, v \cdot p) - \frac{m_X^2 - m_U^2}{m_Y^2 - m_X^2} J_1^{\text{sub}}(m_X, v \cdot p) \right], \quad (23)$$

where m_U is the mass of any of the mesons made up of a sea quark and a sea anti-quark, m_X and m_Y are the masses of the flavor-neutral mesons made up of $x\bar{x}$ and $y\bar{y}$ quarks, respectively, and the function J_1^{sub} , defined below in Eq. (51), is the result of the momentum integral.

⁵ A similar argument will be given in more detail below when discussing Figs. 7 and 8.

The ratios of mass differences in Eq. (23) can be recognized as the residue functions (see Appendix B) for the various poles. For example, $(m_Y^2 - m_U^2)/(m_Y^2 - m_X^2)$ is the residue for the pole at $q^2 = m_Y^2$. These residues are rather simple in this case because of the degeneracy of the sea quarks. To generalize Eq. (23) to the completely non-degenerate case, we simply need to replace the residues by their general expressions. For N_{sea} non-degenerate sea quarks, Eq. (23) is replaced by

$$- \frac{g_\pi^2}{(4\pi f)^2} \frac{1}{N_{\text{sea}}} \sum_j \left[\hat{R}_j^{[N_{\text{sea}}+1, N_{\text{sea}}]} J_1^{\text{sub}}(m_j, v \cdot p) \right], \quad (24)$$

where the Minkowski residues $\hat{R}_j^{[n,k]}$ are defined in Eq. (B2), and the sum over j is over the $N_{\text{sea}} + 1$ mesons that make up the denominator masses in the disconnected propagator after $m_0^2 \rightarrow \infty$. (See Eq. (A21) and the discussion following it.) We leave implicit, for now, the arguments to the residues in Eq. (24); we will be more explicit in the final results below. In addition, we will ultimately express everything in terms of Euclidean-space residues $R_j^{[n,k]}$, Eq. (B4), simply because those are what have been defined and used previously [13, 19].

Cases with double poles present no additional problems, since Ref. [33] shows these explicitly as derivatives with respect to squared masses of the results of single-pole integrals. We will therefore simply get derivatives of the usual residues, as in Eq. (B3).

As discussed above, we will need the expression *before* the $m_0^2 \rightarrow \infty$ limit is taken in order to generalize the result to the disconnected taste-vector and axial-vector cases. Equation (A21) and the fact that $m_{\eta'}^2 \approx N_{\text{sea}} m_0^2/3$ for large m_0 allow us to rewrite Eq. (24) as

$$+ \frac{g_\pi^2}{(4\pi f)^2} \frac{m_0^2}{3} \sum_j \left[\hat{R}_j^{[N_{\text{sea}}+2, N_{\text{sea}}]} J_1^{\text{sub}}(m_j, v \cdot p) \right]. \quad (25)$$

The sum over j now includes the η' . The sign difference between Eqs. (24) and (25) comes from the sign of the mass term in the Minkowski-space η' propagator.

Generalizing Eq. (25) to the staggered case is then straightforward. For the taste-singlet hairpin contributions, we simply replace each continuum pion mass by the mass of the corresponding taste-singlet pion. In other words, we just let $m_j \rightarrow m_{j,I}$ in Eq. (25). Note that, after the staggered fourth root is properly taken into account, the taste-singlet η' mass goes like $N_{\text{sea}} m_0^2/3$ for large m_0 , as it does in the continuum, so one could reverse the process that led to Eq. (25) and use instead Eq. (24) or even Eq. (23) (for degenerate sea-quarks), with $m_j \rightarrow m_{j,I}$ in both cases. Just as for diagrams with connected pion propagators (see

Eq. (20)), there is also a trivial overall factor of $(\xi_5)_{\alpha\beta}/2$, where α and β are the tastes of the heavy-light meson and the current, respectively, and the ξ_5 is due to the pseudoscalar (Goldstone) taste of the outgoing pion.

For the taste-vector and axial-vector disconnected contributions, a little more work is required. We first note that the factor of $m_0^2/3$ in Eq. (25) is simply $\delta'_\Xi/4$ with $\Xi = I$, the strength of the taste-singlet hairpin, Eq. (A9).⁶ For the other tastes we then replace δ'_Ξ by the appropriate hairpin strength from Eq. (A9) and also replace the pion masses: $m_j \rightarrow m_{j,\Xi}$. In addition, there is an overall sign change for this diagram in going from the singlet to the vector or axial-vector tastes. This comes from the fact that the outgoing pion line in Fig. 5(b) lies between the two ends of the disconnected propagator. Using Eq. (A13) and the Feynman rules for the heavy-light propagators and vertices in Appendix A, one sees that the diagram with a taste- Ξ disconnected propagator goes like $(T_\Xi \xi_5 T_\Xi)_{\alpha\beta}$. This leads to a positive sign for $\Xi = I$ but a negative sign for tastes that anticommute with ξ_5 . Finally, the fact that there are four degenerate taste-vector (or axial-vector) pions at this order leads to an additional overall factor of four.

When we attempt to apply the same procedure to the other diagrams in Figs. 4 and 5, we find a further complication in diagrams Fig. 4(a), Fig. 4(b), and Fig. 5(c), where the external pion and one or more internal pions emerge from the same vertex. The problem is that the ordering of the taste matrices at the vertex is not determined by the meson-level diagram (*i.e.*, each diagram can correspond to several orderings), so we do not immediately know the relative sign of taste-vector and axial-vector contributions relative to the singlet contribution. Nevertheless, a quark-flow analysis allows us to identify appropriate “flags” that signal which terms in Ref. [33] come from which orderings at the vertex.

As an example of the procedure in this case, consider Fig. 5(c). The corresponding quark flow diagrams with disconnected pion propagators are shown Fig. 7. In Fig. 7(a), the outgoing pion lies between the two ends of the disconnected propagator. This produces a change in sign of the taste-vector and axial-vector hairpin contributions relative to the taste-singlet one, just as for Fig. 5(b). In Fig. 7(b), on the other hand, the outgoing pion is emitted outside the disconnected propagator, and all the hairpin contributions have the

⁶ The factor of $1/4$ just comes from the different conventional normalization of the generators in the continuum and staggered cases; see Appendix A for further discussion of normalization issues.

same sign. The same is true of the reflected version of Fig. 7(b), which has the outgoing pion emerging from the other side of the vertex.

Fortunately, Figs. 7(a) and (b) are distinguished by their flavor structure, even in the continuum. In Fig. 7(a), the two “external” mesons in the disconnected propagator have different flavors: The one on the left is an X meson (an $x\bar{x}$ bound state); while the one on the right is a Y meson (a $y\bar{y}$ bound state). In Fig. 7(b), both external mesons in the disconnected propagator are Y mesons. Similarly, the reflected version of Fig. 7(b) has two X mesons in the disconnected propagator. This flavor structure is immediately apparent in the results of Ref. [33]. The parts of Fig. 5(c) that come from the quark flow of Fig. 7(a) are proportional to the function called H_1 , which depends on the masses m_X and m_Y (in our notation), as well as the sea-meson mass. The parts of Fig. 5(c) that come from the quark flow of Fig. 7(b) (or its reflected version) are proportional to the function called G_1 , which depends only on the mass m_Y (or m_X) and the sea-meson mass. To generalize the results of Ref. [33] to the staggered case, we thus can use the method outlined above, and simply include an extra minus sign for those taste-vector and axial-vector hairpin contributions proportional to H_1 (relative to the taste-singlet contributions), but not for those proportional to G_1 . This approach also works for the other problematic diagrams, Figs. 4(a) and (b).

The reader may wonder why the complication associated with ordering the taste matrices at the vertices does not occur when the internal pion propagator is connected, but only in the disconnected case. Figure 8 shows possible quark-flow diagrams for Fig. 5(c) with a connected pion propagator. Figure 8(a) cannot occur in our case because we have assumed that x , the light flavor of the heavy-light meson, is different from y , the light flavor of the weak current.⁷ The same reasoning is what allows us to rule out any connected contributions to Fig. 5(b), as mentioned above. Thus all contributions with connected propagators are of the type shown in Fig. 8(b), or its reflected version, and these never have a sign difference between terms with different internal pion tastes.

We note that one can reproduce the SXPT results for light-light [13] and heavy-light [19] mesons by starting from the continuum PQXPT in Refs. [35] or [36], respectively, and following the procedure described above. The computations are in fact slightly more difficult in those cases than in the one at hand, because Refs. [35] and [36] do not explicitly separate

⁷ Equivalently, we have assumed that the outgoing pion is flavor charged.

double-pole from single-pole contributions. It is therefore takes a little work to express the answers from those references in the form of our residue functions, which is the necessary first step before generalizing to the staggered case.

IV. FORM FACTORS FOR $B \rightarrow P$ DECAY

The standard form factor decomposition for the matrix element between a B_x meson and a P_{xy} meson is

$$\langle P_{xy}(p) | \bar{y} \gamma_\mu b | B_x(p_B) \rangle = \left[(p_B + p)_\mu - q_\mu \frac{m_{B_x}^2 - m_{P_{xy}}^2}{q^2} \right] F_+(q^2) + \frac{m_{B_x}^2 - m_{P_{xy}}^2}{q^2} q_\mu F_0(q^2), \quad (26)$$

where $q = p_B - p$ is the momentum transfer. We are suppressing taste indices everywhere, but emphasize that the light pseudoscalar P_{xy} is assumed to be the Goldstone meson (taste ξ_5). In the heavy quark limit, it is more convenient to write this in terms of form factors which are independent of the heavy meson mass

$$\langle P_{xy}(p) | \bar{y} \gamma_\mu b | B_x(v) \rangle_{HQET} = [p_\mu - (v \cdot p) v_\mu] f_p(v \cdot p) + v_\mu f_v(v \cdot p), \quad (27)$$

where v is the four-velocity of the heavy quark, and $v \cdot p$ is the energy of the pion in the heavy meson rest frame. Recall that the QCD heavy meson state and the HQET heavy meson state are related by

$$|B(p_B)\rangle_{QCD} = \sqrt{m_B} |B(v)\rangle_{HQET}. \quad (28)$$

The form factors f_p and f_v are often called f_\perp and f_\parallel , respectively. As discussed in Sec. III, the taste indices are left implicit in Eqs. (26) and (27), as are the trivial overall factors of $(\xi_5/2)_{\alpha\beta}$ in the matrix elements.

The tree-level diagrams for $B_x \rightarrow P_{xy}$ are shown in Fig. 3. Figure 3(a) is the tree-level “point” contribution to f_v , while Fig. 3(b) is the tree-level “pole” contribution to f_p . We have

$$f_v^{\text{tree}}(v \cdot p) = \frac{\kappa}{f}, \quad f_p^{\text{tree}}(v \cdot p) = \frac{\kappa}{f} \frac{g_\pi}{v \cdot p + \Delta^*}, \quad (29)$$

where $\Delta^* = m_{B^*} - m_B$ is the mass difference of the vector and pseudoscalar heavy-light meson masses at leading order in the chiral expansion, *i.e.*, neglecting all effects of light-quark masses. As in Refs. [33, 40], we drop this splitting inside loops, but keep it in the

internal B^* line in the tree-level diagram Fig. 3(b). This forces the tree-level pole in f_p to be at m_{B^*} , the physical point. Dropping Δ^* inside loops is consistent at leading order in HQET, which is the order to which we are working. It would also be consistent, parametrically, to drop Δ^* everywhere. But this would not be convenient, since the m_{B^*} pole is physically important for f_p .

The non-zero diagrams that correct the form factors to one loop are shown in Fig. 4 for f_v and Fig. 5 for f_p . Table I lists the correspondences between these diagrams and those of Ref. [33]. A number of other diagrams, which can arise in principle, vanish identically due to the transverse nature of the B^* propagator, Eq. (A2); these additional diagrams can be found in Ref. [33]. We do not indicate hairpin vertices explicitly in Figs. 4 and 5; the internal pion propagators in these diagrams may be either connected or disconnected.

Before generalizing the results in Ref. [33] to S χ PT, we discuss a subtle issue that affects Fig. 5(a). If the splitting Δ^* is dropped on internal B^* lines in loop diagrams, as is done in Ref. [33], this diagram has a spurious singularity (a double pole) at $v \cdot p = 0$, the edge of the physical region. The singularity arises from the presence of the two B^* lines that are not inside the loop integral and therefore can be on mass shell in the absence of B^* - B splitting. Including Δ^* on all such internal “on-shell” B^* lines (*i.e.*, lines not inside the loops themselves), as is done in Ref. [40], at least pushes the unnatural double pole out of the physical region. We will follow this prescription for including the splitting, but take it one step further. The loop in Fig. 5(a) is a self-energy correction on the internal B^* line. The double pole results from not iterating the self-energy and summing the geometric series. We will follow the more natural course and sum the series; doing so restores a standard single-pole singularity.

There is a further one-loop contribution that can naturally be included in Fig. 5(a). The corresponding tree-level graph, Fig. 3(b), gets two kinds of corrections that are not shown in Fig. 5. One comes simply from the wavefunction renormalizations on the external pion and B lines; we include those terms explicitly below. The second contribution arises from the one-loop shift in the external meson mass. Since this mass shift depends on the flavor of the light quark in the B_x , namely x , we call it $\delta M_x = \Sigma_x(v \cdot k = 0)$, with $\Sigma_x(v \cdot k)$ the self-energy for B_x or B_x^* . Note that Σ_x is the same for both the B_x and the B_x^* , since the splitting Δ^* is dropped inside loops. When the external B_x line in Fig. 3(b) is put on mass-shell at one loop, the denominator of the internal B_y^* propagator changes from $-2(v \cdot p + \Delta^*)$ to

$-2(v \cdot p + \Delta^* - \delta M_x)$. It is convenient to define Δ_{yx}^* as the full splitting between a B_y^* and a B_x :

$$\Delta_{yx}^* \equiv M_{B_y^*} - M_{B_x} = \Delta^* + \delta M_y - \delta M_x \quad (30)$$

The internal B_y^* propagator now becomes $-2(v \cdot p + \Delta_{yx}^* - \delta M_y)$. The contribution from the mass shift may then be combined with the tree-level and Fig. 5(a) contributions to give:

$$f_p^{\text{self}}(v \cdot p) = \frac{\kappa}{f} \frac{g_\pi}{v \cdot p + \Delta_{yx}^* + D(v \cdot p)} , \quad (31)$$

$$D(v \cdot p) \equiv \Sigma_y(v \cdot p) - \Sigma_y(0) , \quad (32)$$

where the subtraction in D comes from the effect of putting the B_x on mass shell, *via* Eq. (30).

The main difference between the approach taken to the spurious singularity of Fig. 5(a) and that of Bećirević *et al.* [33] is that they work to first order in the self-energy in the corresponding diagram (their diagram (7)). Expanding Eq. (31), we find that D is related in the continuum limit to what Ref. [33] calls $\delta f_p^{(7)}$ by

$$D(v \cdot p) = -v \cdot p \delta f_p^{(7)} . \quad (33)$$

Thus we can find the staggered $D(v \cdot p)$ simply by applying the methods of Sec. III to $\delta f_p^{(7)}$.

We can now write down the expressions for the form factors for $B_x \rightarrow P_{xy}$ decay. For the point form factor, f_v , we have

$$\begin{aligned} f_v^{B_x \rightarrow P_{xy}} &= f_v^{\text{tree}} \left[1 + \delta f_v^{B_x \rightarrow P_{xy}} + c_x^v m_x + c_y^v m_y + c_{\text{sea}}^v (m_u + m_d + m_s) \right. \\ &\quad \left. + c_1^v (v \cdot p) + c_2^v (v \cdot p)^2 + c_a^v a^2 \right] , \end{aligned} \quad (34)$$

where f_v^{tree} is given by Eq. (29), and the analytic coefficients c_x^v , c_y^v , ... arise from next-to-leading order (NLO) terms in the heavy-light chiral Lagrangian (see Sec. IV C). The non-analytic pieces, which come from the diagrams shown in Fig. 4 as well as the wavefunction renormalizations, are included in $\delta f_v^{B_x \rightarrow P_{xy}}$:

$$\delta f_v^{B_x \rightarrow P_{xy}} = \delta f_v^{4(a)} + \delta f_v^{4(b)} + \frac{1}{2} \delta Z_{B_x} + \frac{1}{2} \delta Z_{P_{xy}} . \quad (35)$$

The wavefunction renormalization terms, δZ_{B_x} and $\delta Z_{P_{xy}}$, have been calculated previously [13, 19] in SXPT and are listed in Appendix C.

For the f_p form factor, we write

$$f_p^{B_x \rightarrow P_{xy}} = f_p^{\text{self}} + \tilde{f}_p^{\text{tree}} [\delta f_p^{B_x \rightarrow P_{xy}} + c_x^p m_x + c_y^p m_y + c_{\text{sea}}^p (m_u + m_d + m_s) + c_1^p (v \cdot p) + c_2^p (v \cdot p)^2 + c_a^p a^2] . \quad (36)$$

where f_p^{self} is defined in Eq. (31), and

$$\tilde{f}_p^{\text{tree}}(v \cdot p) \equiv \frac{\kappa}{f} \frac{g_\pi}{v \cdot p + \Delta_{xy}^*} . \quad (37)$$

Non-analytic contributions are summarized in the function $D(v \cdot p)$ in f_p^{self} , Eq. (32), and $\delta f_p^{B_x \rightarrow P_{xy}}$, which comes from Figs. 5(b)-(d) and wavefunction renormalizations. Explicitly,

$$\delta f_p^{B_x \rightarrow P_{xy}} = \delta f_p^{5(b)} + \delta f_p^{5(c)} + \delta f_p^{5(d)} + \frac{1}{2} \delta Z_{B_x} + \frac{1}{2} \delta Z_{P_{xy}} . \quad (38)$$

For simplicity, we do not include the superscript $B_x \rightarrow P_{xy}$ on the individual diagrams in Eqs. (35) and (38).

Using $\tilde{f}_p^{\text{tree}}$, which includes the full $B_y^* - B_x$ splitting Δ_{yx}^* , rather than f_p^{tree} , Eq. (29), changes Eq. (36) only by higher-order terms. However, it is convenient to keep the same splitting in both f_p^{self} and the other terms in Eq. (36). Note that it is also consistent at this order to use the alternative form

$$f_p^{B_x \rightarrow P_{xy}} = f_p^{\text{self}} [1 + \delta f_p^{B_x \rightarrow P_{xy}} + c_x^p m_x + c_y^p m_y + c_{\text{sea}}^p (m_u + m_d + m_s) + c_1^p (v \cdot p) + c_2^p (v \cdot p)^2 + c_a^p a^2] , \quad (39)$$

The analytic terms in f_v and f_p are not all independent. As mentioned in Sec. II, there is one relation among the terms that control the valence mass dependence:

$$c_x^p + c_x^v = c_y^p + c_y^v \quad (40)$$

We show that this relation follows from the higher order terms in the Lagrangian and current in Sec. IV C. All other NLO parameters in Eqs. (34) and (36) are independent.

A. Form factors for 3-flavor partially quenched SXPT

First we display the results for the individual diagrams shown in Figs. 4 and 5 for the fully non-degenerate case with three dynamical flavors (the “1+1+1” case). This means

that we have already taken into account the transition from 4 to 1 tastes per flavor. Indeed, our method of generalizing the partially quenched continuum expressions to the staggered case automatically includes this adjustment. We detail below the minor changes needed to obtain 2+1 results from those in the 1+1+1 case.

We first define sets of masses which appear in the numerators and denominators of the disconnected propagators with taste labels implicit (see Appendix B):

$$\mu^{(3)} = \{m_U^2, m_D^2, m_S^2\} , \quad (41)$$

$$\mathcal{M}^{(3,x)} = \{m_X^2, m_{\pi^0}^2, m_\eta^2\} , \quad (42)$$

$$\mathcal{M}^{(4,x)} = \{m_X^2, m_{\pi^0}^2, m_\eta^2, m_{\eta'}^2\} , \quad (43)$$

$$\mathcal{M}^{(4,xy)} = \{m_X^2, m_Y^2, m_{\pi^0}^2, m_\eta^2\} , \quad (44)$$

$$\mathcal{M}^{(5,xy)} = \{m_X^2, m_Y^2, m_{\pi^0}^2, m_\eta^2, m_{\eta'}^2\} . \quad (45)$$

For the mass sets (42) and (43), there are also corresponding sets with $x \rightarrow y$ and $X \rightarrow Y$. When we show explicit taste subscripts such as I or V on the mass sets μ or \mathcal{M} , it means that all the masses in the set have that taste.

The functions that appear in the form factors are⁸

$$I_1(m) = m^2 \ln \left(\frac{m^2}{\Lambda^2} \right) , \quad (46)$$

$$I_2(m, \Delta) = -2\Delta^2 \ln \left(\frac{m^2}{\Lambda^2} \right) - 4\Delta^2 F \left(\frac{m}{\Delta} \right) + 2\Delta^2 , \quad (47)$$

$$J_1(m, \Delta) = \left(-m^2 + \frac{2}{3}\Delta^2 \right) \ln \left(\frac{m^2}{\Lambda^2} \right) + \frac{4}{3}(\Delta^2 - m^2) F \left(\frac{m}{\Delta} \right) - \frac{10}{9}\Delta^2 + \frac{4}{3}m^2 , \quad (48)$$

$$F(x) = \begin{cases} \sqrt{1-x^2} \tanh^{-1} \left(\sqrt{1-x^2} \right) , & 0 \leq x \leq 1 \\ -\sqrt{x^2-1} \tan^{-1} \left(\sqrt{x^2-1} \right) , & x \geq 1 . \end{cases} \quad (49)$$

The main difference in these formulae with those of Bećirević *et al.* [33] is that they keep the divergence pieces, while we have renormalized as in Refs. [13, 19]. To convert to our form, replace the $\overline{\text{MS}}$ scale μ in Ref. [33] with the chiral scale Λ and set their quantity $\bar{\Delta}$ to zero, where

$$\bar{\Delta} \equiv \frac{2}{4-d} - \gamma + \ln(4\pi) + 1 , \quad (50)$$

⁸ For ease of comparison to Ref. [33], we use $I_1(m)$ instead of $\ell(m^2)$ (as in Refs. [13, 19]) for the chiral logarithm.

with d the number of dimensions. $F(x)$ is only needed for positive x ; so we use the simpler form given in Ref. [40], rather than the more general version worked out in Ref. [41] and quoted in Ref. [33]. We do not list the function J_2 , which appears in the integral $\mathcal{J}^{\mu\nu}$ of Eq. (B8) but does not enter the final answers.

We also define a “subtracted” J_1 function by

$$J_1^{\text{sub}}(m, \Delta) \equiv J_1(m, \Delta) - \frac{2\pi m^3}{3\Delta} . \quad (51)$$

The subtraction term cancels the singularity when $\Delta \rightarrow 0$. The function J_1^{sub} enters naturally in the expression for the self energy correction $D(v \cdot p)$ because of the subtraction in Eq. (32). It also turns out to arise from the integral in Fig. 5(b) — see Eq. (26) in Ref. [40].

For the point corrections in the 1+1+1 case, we have

$$\begin{aligned}
\left(\delta f_v^{4(a)}\right)_{1+1+1}^{B_x \rightarrow P_{xy}} &= \frac{1}{2(4\pi f)^2} \left\{ \frac{1}{16} \sum_{f,\Xi} \left[I_1(m_{yf,\Xi}) + 2I_2(m_{yf,\Xi}, v \cdot p) \right] \right. \\
&\quad + \frac{1}{3} \left[\sum_{j \in \mathcal{M}^{(4,xy)}} R_j^{[4,3]} \left(\mathcal{M}_I^{(4,xy)}; \mu_I^{(3)} \right) [I_1(m_{j,I}) + 2I_2(m_{j,I}, v \cdot p)] \right. \\
&\quad \left. + \frac{\partial}{\partial m_{Y,I}^2} \left(\sum_{j \in \mathcal{M}^{(3,y)}} R_j^{[3,3]} \left(\mathcal{M}_I^{(3,y)}; \mu_I^{(3)} \right) [I_1(m_{j,I}) + 2I_2(m_{j,I}, v \cdot p)] \right) \right] \\
&\quad + a^2 \delta'_V \left[\frac{\partial}{\partial m_{Y,V}^2} \left(\sum_{j \in \mathcal{M}^{(4,y)}} R_j^{[4,3]} \left(\mathcal{M}_V^{(4,y)}; \mu_V^{(3)} \right) [I_1(m_{j,V}) + 2I_2(m_{j,V}, v \cdot p)] \right) \right. \\
&\quad \left. - \sum_{j \in \mathcal{M}^{(5,xy)}} R_j^{[5,3]} \left(\mathcal{M}_V^{(5,xy)}; \mu_V^{(3)} \right) [I_1(m_{j,V}) + 2I_2(m_{j,V}, v \cdot p)] \right] \\
&\quad \left. + [V \rightarrow A] \right\}, \tag{52}
\end{aligned}$$

$$\begin{aligned}
\left(\delta f_v^{4(b)}\right)_{1+1+1}^{B_x \rightarrow P_{xy}} &= -\frac{1}{6(4\pi f)^2} \left\{ \frac{1}{16} \sum_{f,\Xi} [I_1(m_{xf,\Xi}) + I_1(m_{yf,\Xi})] \right. \\
&\quad + \frac{1}{3} \left[\frac{\partial}{\partial m_{Y,I}^2} \left(\sum_{j \in \mathcal{M}^{(3,y)}} R_j^{[3,3]} \left(\mathcal{M}_I^{(3,y)}; \mu_I^{(3)} \right) I_1(m_{j,I}) \right) \right. \\
&\quad + \frac{\partial}{\partial m_{X,I}^2} \left(\sum_{j \in \mathcal{M}^{(3,x)}} R_j^{[3,3]} \left(\mathcal{M}_I^{(3,x)}; \mu_I^{(3)} \right) I_1(m_{j,I}) \right) \\
&\quad \left. - \sum_{j \in \mathcal{M}^{(4,xy)}} R_j^{[4,3]} \left(\mathcal{M}_I^{(4,xy)}; \mu_I^{(3)} \right) I_1(m_{j,I}) \right] \\
&\quad + a^2 \delta'_V \left[\frac{\partial}{\partial m_{Y,V}^2} \left(\sum_{j \in \mathcal{M}^{(4,y)}} R_j^{[4,3]} \left(\mathcal{M}_V^{(4,y)}; \mu_V^{(3)} \right) I_1(m_{j,V}) \right) \right. \\
&\quad + \frac{\partial}{\partial m_{X,V}^2} \left(\sum_{j \in \mathcal{M}^{(4,x)}} R_j^{[4,3]} \left(\mathcal{M}_V^{(4,x)}; \mu_V^{(3)} \right) I_1(m_{j,V}) \right) \\
&\quad \left. + \sum_{j \in \mathcal{M}^{(5,xy)}} R_j^{[5,3]} \left(\mathcal{M}_V^{(5,xy)}; \mu_V^{(3)} \right) I_1(m_{j,V}) \right] + [V \rightarrow A] \Big\}. \tag{53}
\end{aligned}$$

Those that correct the pole form factors are

$$\begin{aligned}
(D)_{1+1+1}^{B_x \rightarrow P_{xy}} = & -\frac{3g_\pi^2 v \cdot p}{(4\pi f)^2} \left\{ \frac{1}{16} \sum_{f, \Xi} J_1^{\text{sub}}(m_{yf, \Xi}, v \cdot p) \right. \\
& + \frac{1}{3} \sum_{j \in \mathcal{M}^{(3, y)}} \frac{\partial}{\partial m_{Y, I}^2} \left[R_j^{[3, 3]} \left(\mathcal{M}_I^{(3, y)}; \mu_I^{(3)} \right) J_1^{\text{sub}}(m_{j, I}, v \cdot p) \right] \\
& + a^2 \delta'_V \sum_{j \in \mathcal{M}^{(4, y)}} \frac{\partial}{\partial m_{Y, V}^2} \left[R_j^{[4, 3]} \left(\mathcal{M}_V^{(4, y)}; \mu_V^{(3)} \right) J_1^{\text{sub}}(m_{j, V}, v \cdot p) \right] \\
& \left. + [V \rightarrow A] \right\}, \tag{54}
\end{aligned}$$

$$\begin{aligned}
\left(\delta f_p^{5(b)} \right)_{1+1+1}^{B_x \rightarrow P_{xy}} = & \frac{g_\pi^2}{(4\pi f)^2} \left\{ -\frac{1}{3} \sum_{j \in \mathcal{M}^{(4, xy)}} R_j^{[4, 3]} \left(\mathcal{M}_I^{(4, xy)}; \mu_I^{(3)} \right) J_1^{\text{sub}}(m_{j, I}, v \cdot p) \right. \\
& \left. + a^2 \delta'_V \sum_{j \in \mathcal{M}^{(5, xy)}} R_j^{[5, 3]} \left(\mathcal{M}_V^{(5, xy)}; \mu_V^{(3)} \right) J_1^{\text{sub}}(m_{j, V}, v \cdot p) + [V \rightarrow A] \right\}, \tag{55}
\end{aligned}$$

$$\begin{aligned}
\left(\delta f_p^{5(c)} \right)_{1+1+1}^{B_x \rightarrow P_{xy}} = & -\frac{1}{6(4\pi f)^2} \left\{ \frac{1}{16} \sum_{f, \Xi} [I_1(m_{xf, \Xi}) + I_1(m_{yf, \Xi})] \right. \\
& + \frac{1}{3} \left[\sum_{j \in \mathcal{M}^{(3, y)}} \frac{\partial}{\partial m_{Y, I}^2} \left[R_j^{[3, 3]} \left(\mathcal{M}_I^{(3, y)}; \mu_I^{(3)} \right) I_1(m_{j, I}) \right] \right. \\
& + \sum_{j \in \mathcal{M}^{(3, x)}} \frac{\partial}{\partial m_{X, I}^2} \left[R_j^{[3, 3]} \left(\mathcal{M}_I^{(3, x)}; \mu_I^{(3)} \right) I_1(m_{j, I}) \right] \\
& + 2 \sum_{j \in \mathcal{M}^{(4, xy)}} \left[R_j^{[4, 3]} \left(\mathcal{M}_I^{(4, xy)}; \mu_I^{(3)} \right) I_1(m_{j, I}) \right] \\
& + a^2 \delta'_V \left[\sum_{j \in \mathcal{M}^{(4, y)}} \frac{\partial}{\partial m_{Y, V}^2} \left[R_j^{[4, 3]} \left(\mathcal{M}_V^{(4, y)}; \mu_V^{(3)} \right) I_1(m_{j, V}) \right] \right. \\
& + \sum_{j \in \mathcal{M}^{(4, x)}} \frac{\partial}{\partial m_{X, V}^2} \left[R_j^{[4, 3]} \left(\mathcal{M}_V^{(4, x)}; \mu_V^{(3)} \right) I_1(m_{j, V}) \right] \\
& \left. \left. - 2 \sum_{j \in \mathcal{M}^{(5, xy)}} \left[R_j^{[5, 3]} \left(\mathcal{M}_V^{(5, xy)}; \mu_V^{(3)} \right) I_1(m_{j, V}) \right] \right] + [V \rightarrow A] \right\}, \tag{56}
\end{aligned}$$

$$\begin{aligned}
\left(\delta f_p^{5(d)} \right)_{1+1+1}^{B_x \rightarrow P_{xy}} = & -\frac{1}{2(4\pi f)^2} \left\{ \frac{1}{16} \sum_{f, \Xi} I_1(m_{yf, \Xi}) \right. \\
& + \frac{1}{3} \sum_{j \in \mathcal{M}^{(3, y)}} \frac{\partial}{\partial m_{Y, I}^2} \left[R_j^{[3, 3]} \left(\mathcal{M}_I^{(3, y)}; \mu_I^{(3)} \right) I_1(m_{j, I}) \right] \\
& \left. + a^2 \delta'_V \sum_{j \in \mathcal{M}^{(4, y)}} \frac{\partial}{\partial m_{Y, V}^2} \left[R_j^{[4, 3]} \left(\mathcal{M}_V^{(4, y)}; \mu_V^{(3)} \right) I_1(m_{j, V}) \right] + [V \rightarrow A] \right\}. \tag{57}
\end{aligned}$$

In Eqs. (52) through (57), the explicit factors of $1/3$ in front of terms involving the taste-singlet (I) mesons come from the factors of $1/N_{\text{sea}}$ in Ref. [33].

To get the full corrections for both f_v and f_p , we need to add in the wavefunction renormalizations, given in Appendix C in Eqs. (35) and (38). Putting these together with the analytic terms and (for f_p) the D term, Eqs. (34) and (36) give the complete NLO expressions for the form factors in SXPT.

The above 1+1+1 results are expressed in terms of the Euclidean residue functions $R_j^{[n,k]}$, Eq. (B4). In the 2+1 case, there is a cancellation in the residues between the contribution of the U or D in the numerator and that of the π_0 in the denominator. Thus, to obtain the 2+1 from the 1+1+1 case, one must simply reduce by one all superscripts on the residues, *i.e.*, $R^{[n,k]} \rightarrow R^{[n-1,k-1]}$, and remove m_{π_0} and (say) m_D from the mass sets:

$$\mu^{(3)} \rightarrow \{m_U^2, m_S^2\} , \quad (58)$$

$$\mathcal{M}^{(3,x)} \rightarrow \{m_X^2, m_\eta^2\} , \quad (59)$$

$$\mathcal{M}^{(4,x)} \rightarrow \{m_X^2, m_\eta^2, m_{\eta'}^2\} , \quad (60)$$

$$\mathcal{M}^{(4,xy)} \rightarrow \{m_X^2, m_Y^2, m_\eta^2\} , \quad (61)$$

$$\mathcal{M}^{(5,xy)} \rightarrow \{m_X^2, m_Y^2, m_\eta^2, m_{\eta'}^2\} . \quad (62)$$

We also write here the expressions for three non-degenerate dynamical flavors in continuum PQχPT, which to our knowledge do not appear in the literature. These expressions can be obtained either by returning to Ref. [33] and using the residue functions to generalize to the non-degenerate case, or simply by taking the continuum limit of the above equations.

Either way, the results for f_v are

$$\begin{aligned}
\left(\delta f_v^{4(a),\text{cont}}\right)^{B_x \rightarrow P_{xy}} &= \frac{1}{2(4\pi f)^2} \left\{ \sum_f \left[I_1(m_{yf}) + 2I_2(m_{yf}, v \cdot p) \right] \right. \\
&\quad + \frac{1}{3} \left[\sum_{j \in \mathcal{M}^{(4,xy)}} R_j^{[4,3]}(\mathcal{M}^{(4,xy)}; \mu^{(3)}) [I_1(m_j) + 2I_2(m_j, v \cdot p)] \right. \\
&\quad \left. \left. + \frac{\partial}{\partial m_Y^2} \left(\sum_{j \in \mathcal{M}^{(3,y)}} R_j^{[3,3]}(\mathcal{M}^{(3,y)}; \mu^{(3)}) [I_1(m_j) + 2I_2(m_j, v \cdot p)] \right) \right] \right\}, \\
\left(\delta f_v^{4(b),\text{cont}}\right)^{B_x \rightarrow P_{xy}} &= -\frac{1}{6(4\pi f)^2} \left\{ \sum_f [I_1(m_{xf}) + I_1(m_{yf})] \right. \\
&\quad + \frac{1}{3} \left[\frac{\partial}{\partial m_Y^2} \left(\sum_{j \in \mathcal{M}^{(3,y)}} R_j^{[3,3]}(\mathcal{M}^{(3,y)}; \mu^{(3)}) I_1(m_j) \right) \right. \\
&\quad + \frac{\partial}{\partial m_X^2} \left(\sum_{j \in \mathcal{M}^{(3,x)}} R_j^{[3,3]}(\mathcal{M}^{(3,x)}; \mu^{(3)}) I_1(m_j) \right) \\
&\quad \left. \left. - \sum_{j \in \mathcal{M}^{(4,xy)}} R_j^{[4,3]}(\mathcal{M}^{(4,xy)}; \mu^{(3)}) I_1(m_j) \right] \right\}, \tag{63}
\end{aligned}$$

while those for f_p are

$$\begin{aligned}
(D^{\text{cont}})^{B_x \rightarrow P_{xy}} &= -\frac{3g_\pi^2 v \cdot p}{(4\pi f)^2} \left\{ \sum_f J_1^{\text{sub}}(m_{yf}, v \cdot p) \right. \\
&\quad \left. + \frac{1}{3} \sum_{j \in \mathcal{M}^{(3,y)}} \frac{\partial}{\partial m_Y^2} \left[R_j^{[3,3]}(\mathcal{M}^{(3,y)}; \mu^{(3)}) J_1^{\text{sub}}(m_j, v \cdot p) \right] \right\}, \\
(\delta f_p^{5(b), \text{cont}})^{B_x \rightarrow P_{xy}} &= \frac{g_\pi^2}{(4\pi f)^2} \left\{ -\frac{1}{3} \sum_{j \in \mathcal{M}^{(4,xy)}} R_j^{[4,3]}(\mathcal{M}^{(4,xy)}; \mu^{(3)}) J_1^{\text{sub}}(m_j, v \cdot p) \right\}, \\
(\delta f_p^{5(c), \text{cont}})^{B_x \rightarrow P_{xy}} &= -\frac{1}{6(4\pi f)^2} \left\{ \sum_f [I_1(m_{xf}) + I_1(m_{yf})] \right. \\
&\quad + \frac{1}{3} \left[\sum_{j \in \mathcal{M}^{(3,y)}} \frac{\partial}{\partial m_Y^2} \left[R_j^{[3,3]}(\mathcal{M}^{(3,y)}; \mu^{(3)}) I_1(m_j) \right] \right. \\
&\quad + \sum_{j \in \mathcal{M}^{(3,x)}} \frac{\partial}{\partial m_X^2} \left[R_j^{[3,3]}(\mathcal{M}^{(3,x)}; \mu^{(3)}) I_1(m_j) \right] \\
&\quad \left. \left. + 2 \sum_{j \in \mathcal{M}^{(4,xy)}} \left[R_j^{[4,3]}(\mathcal{M}^{(4,xy)}; \mu^{(3)}) I_1(m_j) \right] \right] \right\}, \\
(\delta f_p^{5(d), \text{cont}})^{B_x \rightarrow P_{xy}} &= -\frac{1}{2(4\pi f)^2} \left\{ \sum_f I_1(m_{yf}) \right. \\
&\quad \left. + \frac{1}{3} \sum_{j \in \mathcal{M}^{(3,y)}} \frac{\partial}{\partial m_Y^2} \left[R_j^{[3,3]}(\mathcal{M}^{(3,y)}; \mu^{(3)}) I_1(m_j) \right] \right\}. \tag{64}
\end{aligned}$$

Corresponding continuum-limit results for the wave-function renormalizations are given in Appendix C.

B. Full QCD Results

Adding together the complete results for the “full QCD” case is straightforward. For simplicity, we specialize to case $m_u = m_d$ (*i.e.*, $2+1$). For $B \rightarrow \pi$, the complete corrections

(including wave-function renormalization) are:

$$\begin{aligned}
D^{B \rightarrow \pi} = & -\frac{3g_\pi^2 v \cdot p}{(4\pi f)^2} \left\{ \frac{1}{16} \sum_{\Xi} [2J_1^{\text{sub}}(m_{\pi, \Xi}, v \cdot p) + J_1^{\text{sub}}(m_{K, \Xi}, v \cdot p)] \right. \\
& - \frac{1}{2} J_1^{\text{sub}}(m_{\pi, I}, v \cdot p) + \frac{1}{6} J_1^{\text{sub}}(m_{\eta, I}, v \cdot p) \\
& + \sum_{j \in \{\pi, \eta, \eta'\}} \left[(-a^2 \delta'_V) R_j^{[3,1]}(\{m_{\pi, V}, m_{\eta, V}, m_{\eta', V}\}; \{m_{S, V}\}) J_1^{\text{sub}}(m_{j, V}, v \cdot p) \right] \\
& \left. + [V \rightarrow A] \right\}, \tag{65}
\end{aligned}$$

$$\begin{aligned}
\delta f_p^{B \rightarrow \pi} = & \frac{1}{(4\pi f)^2} \left\{ \frac{1}{16} \sum_{\Xi} \left[-\frac{1+3g_\pi^2}{2} [2I_1(m_{\pi, \Xi}) + I_1(m_{K, \Xi})] \right] \right. \\
& - \frac{1}{2} g_\pi^2 J_1^{\text{sub}}(m_{\pi, I}, v \cdot p) + \frac{1}{6} g_\pi^2 J_1^{\text{sub}}(m_{\eta, I}, v \cdot p) + \frac{1+3g_\pi^2}{12} [3I_1(m_{\pi, I}) - I_1(m_{\eta, I})] \\
& + \sum_{j \in \{\pi, \eta, \eta'\}} \left[a^2 \delta'_V R_j^{[3,1]}(\{m_{\pi, V}, m_{\eta, V}, m_{\eta', V}\}; \{m_{S, V}\}) \right. \\
& \left. \times \left(g_\pi^2 J_1^{\text{sub}}(m_{j, V}, v \cdot p) + \frac{1+3g_\pi^2}{2} I_1(m_{j, V}) \right) \right] + [V \rightarrow A] \left. \right\}, \tag{66}
\end{aligned}$$

$$\begin{aligned}
\delta f_v^{B \rightarrow \pi} = & \frac{1}{(4\pi f)^2} \left\{ \frac{1}{16} \sum_{\Xi} \left[\frac{1-3g_\pi^2}{2} [2I_1(m_{\pi, \Xi}) + I_1(m_{K, \Xi})] \right. \right. \\
& + 2I_2(m_{\pi, \Xi}, v \cdot p) + I_2(m_{K, \Xi}, v \cdot p) \left. \right] \\
& + \frac{1+3g_\pi^2}{4} \left[I_1(m_{\pi, I}) - \frac{1}{3} I_1(m_{\eta, I}) \right] \\
& + \sum_{j \in \{\pi, \eta, \eta'\}} \left[a^2 \delta'_V R_j^{[3,1]}(\{m_{\pi, V}, m_{\eta, V}, m_{\eta', V}\}; \{m_{S, V}\}) \right. \\
& \left. \times \left(\frac{3(g_\pi^2 - 1)}{2} I_1(m_{j, V}) - 2I_2(m_{j, V}, v \cdot p) \right) \right] + [V \rightarrow A] \left. \right\}. \tag{67}
\end{aligned}$$

For $B \rightarrow K$,⁹ we have

$$\begin{aligned}
D^{B \rightarrow K} = & -\frac{3g_\pi^2(v \cdot p)}{(4\pi f)^2} \left\{ \frac{1}{16} \sum_{\Xi} [2J_1^{\text{sub}}(m_{K,\Xi}, v \cdot p) + J_1^{\text{sub}}(m_{S,\Xi}, v \cdot p)] \right. \\
& + \frac{2}{3} J_1^{\text{sub}}(m_{\eta,I}, v \cdot p) - J_1^{\text{sub}}(m_{S,I}, v \cdot p) \\
& + \sum_{j \in \{S, \eta, \eta'\}} \left[(-a^2 \delta'_V) R_j^{[3,1]}(\{m_{S,V}, m_{\eta,V}, m_{\eta',V}\}; \{m_{\pi,V}\}) J_1^{\text{sub}}(m_{j,V}, v \cdot p) \right] \\
& \left. + [V \rightarrow A] \right\}, \tag{68}
\end{aligned}$$

$$\begin{aligned}
\delta f_p^{B \rightarrow K} = & \frac{1}{(4\pi f)^2} \left\{ \frac{1}{16} \sum_{\Xi} \left[-\frac{2+3g_\pi^2}{2} I_1(m_{K,\Xi}) - \frac{1}{2} I_1(m_{S,\Xi}) - 3g_\pi^2 I_1(m_{\pi,\Xi}) \right] \right. \\
& - \frac{1}{3} g_\pi^2 J_1^{\text{sub}}(m_{\eta,I}, v \cdot p) + \frac{3g_\pi^2}{4} I_1(m_{\pi,I}) - \frac{4+3g_\pi^2}{12} I_1(m_{\eta,I}) + \frac{1}{2} I_1(m_{S,I}) \\
& + a^2 \delta'_V \left[\frac{g_\pi^2}{m_{\eta',V}^2 - m_{\eta,V}^2} \left(J_1^{\text{sub}}(m_{\eta,V}, v \cdot p) - J_1^{\text{sub}}(m_{\eta',V}, v \cdot p) \right) \right. \\
& + \frac{3g_\pi^2}{2} \sum_{j \in \{\pi, \eta, \eta'\}} R_j^{[3,1]}(\{m_{\pi,V}, m_{\eta,V}, m_{\eta',V}\}; \{m_{S,V}\}) I_1(m_{j,V}) \\
& \left. + \frac{1}{2} \sum_{j \in \{S, \eta, \eta'\}} R_j^{[3,1]}(\{m_{S,V}, m_{\eta,V}, m_{\eta',V}\}; \{m_{\pi,V}\}) I_1(m_{j,V}) \right] \\
& \left. + [V \rightarrow A] \right\}, \tag{69}
\end{aligned}$$

⁹ The transition $B \rightarrow K$ occurs through penguin diagrams; $D \rightarrow K$ is a standard semileptonic decay due to the current in Eq. (18). We keep the notation $B \rightarrow K$ however to stress that we are working to lowest order in the heavy quark mass.

$$\begin{aligned}
\delta f_v^{B \rightarrow K} = & \frac{1}{(4\pi f)^2} \left\{ \frac{1}{16} \sum_{\Xi} \left[\frac{2 - 3g_\pi^2}{2} I_1(m_{K,\Xi}) - 3g_\pi^2 I_1(m_{\pi,\Xi}) + \frac{1}{2} I_1(m_{S,\Xi}) \right. \right. \\
& + 2I_2(m_{K,\Xi}, v \cdot p) + I_2(m_{S,\Xi}, v \cdot p) \left. \right] \\
& - \frac{1}{2} I_1(m_{S,I}) + \frac{3g_\pi^2}{4} I_1(m_{\pi,I}) + \frac{8 - 3g_\pi^2}{12} I_1(m_{\eta,I}) + I_2(m_{\eta,I}, v \cdot p) - I_2(m_{S,I}, v \cdot p) \\
& + a^2 \delta'_V \left[\frac{I_1(m_{\eta',V}) - I_1(m_{\eta,V}) + I_2(m_{\eta',V}, v \cdot p) - I_2(m_{\eta,V}, v \cdot p)}{m_{\eta',V}^2 - m_{\eta,V}^2} \right. \\
& - \sum_{j \in \{S, \eta, \eta'\}} R_j^{[3,1]}(\{m_{S,V}, m_{\eta,V}, m_{\eta',V}\}; \{m_{\pi,V}\}) \left(\frac{1}{2} I_1(m_{j,V}) + I_2(m_{j,V}, v \cdot p) \right) \\
& + \frac{3g_\pi^2}{2} \sum_{j \in \{\pi, \eta, \eta'\}} R_j^{[3,1]}(\{m_{\pi,V}, m_{\eta,V}, m_{\eta',V}\}; \{m_{S,V}\}) I_1(m_{j,V}) \left. \right] \\
& \left. + [V \rightarrow A] \right\}. \tag{70}
\end{aligned}$$

C. Analytic terms

From the power counting discussed in Sec. II, as well as interchange symmetry among the sea quark masses, the form factors at the order we are working can only depend only on the valence quark masses m_x and m_y , the sum of the sea quark masses $m_u + m_d + m_s$, the pion momentum (through $v \cdot p$), and the lattice spacing, a . The last must appear quadratically, since the errors of the staggered action are $\mathcal{O}(a^2)$. Recall that we do not include any discretization errors coming from the heavy quark in our effective theory.

Thus we expect to have the analytic terms shown in Eqs. (34) and (36) with coefficients c_i^p and c_i^v . (Here $i = \{x, y, \text{sea}, 1, 2, a\}$.) We then can examine, one by one, the known NLO terms in the Lagrangian and current to check for the existence of relations among the c_i^p and/or c_i^v . As soon as a sufficient number of terms are checked to ensure that the parameters are independent, we are done. It is therefore not necessary in all cases to have a complete catalog of NLO terms. Unless otherwise indicated, all NLO terms discussed in this section come from Ref. [19].

Note first of all that we do not need to include explicitly the effects of mass-renormalization terms in the NLO heavy-light Lagrangian, such as

$$2\lambda_1 \text{Tr}(\overline{H} H \mathcal{M}^+) + 2\lambda'_1 \text{Tr}(\overline{H} H) \text{Tr}(\mathcal{M}^+) , \tag{71}$$

where we define

$$\mathcal{M}^\pm = \frac{1}{2} (\sigma \mathcal{M} \sigma \pm \sigma^\dagger \mathcal{M} \sigma^\dagger) . \quad (72)$$

The effect of the terms in Eq. (71) is absorbed into the $B_y^*-B_x$ mass difference Δ_{yx}^* , Eq. (30), just like the one-loop contribution to the mass. Corresponding $\mathcal{O}(a^2)$ term in the Lagrangian, which can be obtained by replacing \mathcal{M}^+ above by various taste-violating operators, can likewise be ignored here.

We now consider the discretization corrections parametrized by c_a^p and c_a^v . There are a large number of $\mathcal{O}(a^2)$ corrections to the Lagrangian and the current that can contribute to these coefficients, so it is not surprising that they are independent. For example, consider the following terms in the NLO heavy-light Lagrangian

$$a^2 \sum_{k=1}^8 c_{3,k}^A \text{Tr} \left(\overline{H} H \gamma_\mu \gamma_5 \{ \mathbb{A}^\mu, \mathcal{O}_k^{A,+} \} \right) , \quad (73)$$

where the $\mathcal{O}_k^{A,+}$ are various taste-violating operators, similar to those in Eq. (16) above. These terms do not contribute to c_a^v , but only to c_a^p , though corrections to the B - B^* - π vertex in Fig. 3(b). On the other hand, there are many terms that contribute both to c_a^v and to c_a^p . An example is the following correction to the current

$$a^2 \sum_{k=1}^8 r_{1,k}^A \text{tr}_D (\gamma^\mu (1 - \gamma_5) H) \mathcal{O}_k^{A,+} \sigma^\dagger \lambda^{(b)} , \quad (74)$$

which contributes equally to c_a^v and c_a^p . Additional examples are provided by those terms with two derivatives in the $\mathcal{O}(m_q a^2)$ pion Lagrangian [39], which correct both coefficients though their effect on the pion wave-function renormalization.

We consider the $v \cdot p$ and $(v \cdot p)^2$ terms next, namely c_1^v , c_2^v , c_1^p , and c_2^p . This is a case where a complete catalog of Lagrangian and current corrections does not exist. However, it is easy to find corrections that contribute only to f_v or only to f_p . As in the previous case, corrections to the B - B^* - π vertex in Fig. 3(b) only affect f_p at the order we are working. Thus,

$$\frac{i\epsilon_1}{\Lambda_\chi} \text{Tr} \left((v \cdot \overrightarrow{D} \overline{H} H - \overline{H} H v \cdot \overleftarrow{D}) \gamma_\mu \gamma_5 \mathbb{A}^\mu \right) \quad (75)$$

contributes to c_1^p only; while

$$\frac{\epsilon_3}{\Lambda_\chi^2} \text{Tr} \left(\overline{H} H \gamma_\mu \gamma_5 (v \cdot \overrightarrow{D})^2 \mathbb{A}^\mu \right) \quad (76)$$

contributes to c_2^p only. Similarly, only f_v is affected, though Fig. 3(a), by any correction to the current whose expansion in terms of pion fields starts at linear order (*i.e.*, corrections of schematic form $H(\frac{i\Phi}{2f} + \dots)$, with \dots denoting higher order terms in Φ). Thus,

$$\frac{\kappa_2}{\Lambda_\chi} \text{tr}_D(\gamma^\mu (1 - \gamma_5) H) v \cdot \mathbb{A} \sigma^\dagger \lambda^{(b)} \quad (77)$$

contributes to c_1^v only; while

$$\frac{i\kappa_4}{\Lambda_\chi^2} \text{tr}_D(\gamma^\mu (1 - \gamma_5) H) v \cdot \vec{D} v \cdot \mathbb{A} \sigma^\dagger \lambda^{(b)} \quad (78)$$

contributes to c_2^v only. Since there is at least one Lagrangian or current term that contributes to each of c_1^v , c_2^v , c_1^p , and c_2^p exclusively, these coefficients are independent.

The argument for the independence of the sea-quark mass terms, *i.e.*, the coefficients c_{sea}^v and c_{sea}^p , is similar. The Lagrangian correction

$$k_4 \text{Tr}(\overline{H} H \gamma_\mu \gamma_5 \mathbb{A}^\mu) \text{Tr}(\mathcal{M}^+) \quad (79)$$

contributes to c_{sea}^p only; while the current correction

$$\rho_2 \text{tr}_D(\gamma^\mu (1 - \gamma_5) H) \sigma^\dagger \lambda^{(b)} \text{Tr}(\mathcal{M}^+) \quad (80)$$

contributes equally to both c_{sea}^p and c_{sea}^v . These two observations are enough to guarantee that c_{sea}^v and c_{sea}^p are independent.

We now turn to the coefficients that control the valence quark mass dependence of the form factors: c_x^v , c_y^v , c_x^p , and c_y^p . At first glance, it would seem unlikely that there could be any constraint among these parameters, since there are seven terms in the Lagrangian and current in Ref. [19] that could generate valence mass dependence.¹⁰ However, three of these terms are immediately eliminated, either because they could only contribute to flavor-neutral pions (with $x = y$), or because they produce no fewer than two pions. There are then two remaining corrections to the heavy-light Lagrangian,

$$ik_1 \text{Tr}(\overline{H} H v \cdot \overleftarrow{D} \mathcal{M}^+ - v \cdot \overrightarrow{D} \overline{H} H \mathcal{M}^+) + k_3 \text{Tr}(\overline{H} H \gamma_\mu \gamma_5 \{\mathbb{A}^\mu, \mathcal{M}^+\}) \quad (81)$$

and two corrections to the current,

$$\rho_1 \text{tr}_D(\gamma^\mu (1 - \gamma_5) H) \mathcal{M}^+ \sigma^\dagger \lambda^{(b)} + \rho_3 \text{tr}_D(\gamma^\mu (1 - \gamma_5) H) \mathcal{M}^- \sigma^\dagger \lambda^{(b)} \quad (82)$$

¹⁰ There are additional terms involving $\text{Tr}(\mathcal{M}^+)$, as in Eqs. (79) and (80), that only give sea quark mass dependence at this order.

The k_3 term in Eq. (81) contributes only to f_p , through the B - B^* - π vertex. However, because of the anticommutator, its contribution is proportional to $m_x + m_y$, so it gives equal contributions to c_x^p and c_y^p . Similarly, because the one-pion term in \mathcal{M}^- is proportional to $\Phi\mathcal{M} + \mathcal{M}\Phi$, the ρ_3 term contributes equally to c_x^v and c_y^v (but not at all to c_x^p and c_y^p). Further, since \mathcal{M}^+ creates only even number of pions, we can replace it by \mathcal{M} in Eq. (82). The ρ_1 term can then easily be seen to contribute equally to c_y^p and c_x^v , since the current needs to annihilate a B_y^* in the f_p case and a B_x in the f_v case.

The contributions of the k_1 term in Eq. (81) are the most non-trivial. It contributes to both c_x^v and c_x^p through wave function renormalization on the external B_x line, but it also contributes to c_y^p through an insertion on the internal B_y^* line in Fig. 3(b). However, since wave-function renormalization effects on external lines go like \sqrt{Z} , the contributions of this term to both c_x^v and c_x^p are exactly half of its contribution to c_y^p . Thus, all four terms in Eqs. (81) and (82) are consistent with the relation given in Eq. (40).

We still need to worry about valence mass dependence generated by the standard $\mathcal{O}(p^4)$ pion Lagrangian [38] through wave function renormalization of the external pion. Such contributions do exist (from L_5), but the $x \leftrightarrow y$ symmetry of the pion guarantees they are proportional to $m_x + m_y$ in both f_p and f_v , and hence do not violate Eq. (40).

A consistency check of the relation, Eq. (40), as well as of the claimed independence of the other analytic terms, can be performed by considering the change in the chiral logarithms in Eqs. (52) through (57) and Eqs. (C1) and (C2) under a change in chiral scale. To simplify the calculation, it is very convenient to use the conditions obeyed by sums of residues, which are given in Eq. (38) of the second paper in Ref. [13]. We find that such a scale change can be absorbed by parameters that obey Eq. (40) but are otherwise independent.

In the continuum limit, c_{sea}^p and c_{sea}^v remain independent, as do c_1^p , c_2^p , c_1^v , and c_2^v . We disagree on these points with Ref. [33], which found $c_{\text{sea}}^p = c_{\text{sea}}^v$, and did not consider analytic terms giving $v \cdot p$ dependence. The difference can be traced to the inclusion here of the effects of the complete set of NLO mass-dependent terms, as well as a sufficient number of higher derivative terms (Eqs. (75) through (78)). In particular, the independence of c_{sea}^p and c_{sea}^v can be traced to the existence of the Lagrangian correction, Eq. (79), which was not considered in Ref. [33]. On the other hand, the relation among the valence mass coefficients, Eq. (40), is obeyed by the expressions for these coefficients found in Ref. [33]. This occurs because the contributions of the terms proportional to k_3 and ρ_3 in Eqs. (81) and (82), which were

not considered in Ref. [33], are proportional to $m_x + m_y$ and automatically obey Eq. (40).

Note, finally, that the relation in Eq. (40) is almost certain to be violated at next order in HQET. This is because the contributions from operators like the k_1 term in Eq. (81) will affect the B and the B^* differently at $\mathcal{O}(1/m_Q)$, destroying the cancellation that made Eq. (40) possible.

V. FINITE VOLUME EFFECTS

In a finite volume, we must replace the integrals in Eqs. (B5) through (B8) by discrete momentum sums. We assume that the time direction is large enough to be considered infinite (this is the case in MILC simulations), and that each of the spatial lengths has (dimensionful) size L .

The correction to Eq. (B5) is given explicitly in Ref. [12]. In finite volume, we need only make the replacement

$$I_1(m) \rightarrow I_1^{\text{fv}}(m) = I_1(m) + m^2 \delta_1(mL) . \quad (83)$$

Here δ_1 is a sum over modified Bessel functions

$$\delta_1(mL) = \frac{4}{mL} \sum_{\vec{r} \neq 0} \frac{K_1(rmL)}{r} , \quad (84)$$

where \vec{r} is a 3-vector with integer components, and $r \equiv |\vec{r}|$.

Arndt and Lin [42] have worked out the finite volume correction to Eq. (B6). In our notation, the function $I_2(m, \Delta)$ is replaced by its finite volume form, $I_2^{\text{fv}}(m, \Delta)$,

$$I_2(m, \Delta) \rightarrow I_2^{\text{fv}}(m, \Delta) = I_2(m, \Delta) + \delta I_2(m, \Delta, L) , \quad (85)$$

where the correction $\delta I_2(m, \Delta, L)$ is given simply in terms of the function $J_{\text{FV}}(m, \Delta, L)$ defined in Eq. (44) of Ref. [42]:¹¹

$$\begin{aligned} \delta I_2(m, \Delta, L) &= -(4\pi)^2 \Delta J_{\text{FV}}(m, \Delta, L) \\ J_{\text{FV}}(m, \Delta, L) &\equiv \left(\frac{1}{2\pi} \right)^2 \sum_{\vec{r} \neq 0} \int_0^\infty dq \left(\frac{q}{\omega_q(\omega_q + \Delta)} \right) \left(\frac{\sin(qrL)}{rL} \right) , \end{aligned} \quad (86)$$

¹¹ We have added the L argument to J_{FV} for consistency with our notation

with $\omega_q = \sqrt{q^2 + m^2}$.

The asymptotic form of $J_{\text{FV}}(m, \Delta, L)$ for large mL is useful for practical applications, where typically $mL > 3$, and often $mL > 4$ [8, 9]. Arndt and Lin have found [42]:

$$J_{\text{FV}}(m, \Delta, L) = \sum_{\vec{r} \neq 0} \left(\frac{1}{8\pi r L} \right) e^{-rmL} \mathcal{A}, \quad (87)$$

$$\begin{aligned} \mathcal{A} = & e^{(z^2)} [1 - \text{Erf}(z)] + \left(\frac{1}{rmL} \right) \left[\frac{1}{\sqrt{\pi}} \left(\frac{z}{4} - \frac{z^3}{2} \right) + \frac{z^4}{2} e^{(z^2)} [1 - \text{Erf}(z)] \right] \\ & - \left(\frac{1}{rmL} \right)^2 \left[\frac{1}{\sqrt{\pi}} \left(\frac{9z}{64} - \frac{5z^3}{32} + \frac{7z^5}{16} + \frac{z^7}{8} \right) - \left(\frac{z^6}{2} + \frac{z^8}{8} \right) e^{(z^2)} [1 - \text{Erf}(z)] \right] \\ & + \mathcal{O} \left(\frac{1}{(rmL)^3} \right), \end{aligned} \quad (88)$$

where

$$z \equiv \left(\frac{\Delta}{m} \right) \sqrt{\frac{rmL}{2}}. \quad (89)$$

Computing higher orders in the $1/(mL)$ expansion is possible if greater precision is needed.

Since the functions $I_1(m)$ and $I_2(m, \Delta)$ arise from the integral $\mathcal{I}_3^\mu(m, \Delta)$ in Eq. (B7), as well as from Eqs. (B5) and (B6), which serve to define them, it is necessary to check that the finite volume corrections coming from Eq. (B7) are just those given by Eqs. (83) and (85) above. This is easily seen to be true in the rest frame of the heavy quark, in which we are working. It is a consequence of the facts that: (1) in the rest frame, only the $\mu = 0$ component of $\mathcal{I}_3^\mu(m, \Delta)$ is non-zero, and (2) the integral over dq^0 is unaffected by finite volume, since we assume large time-extent of the lattices. The finite volume integral then splits into $I_1^{\text{fv}}(m)$ and $I_2^{\text{fv}}(m, \Delta)$ pieces, just as in infinite volume.

Finally, we have to examine the finite volume corrections to the integral $\mathcal{J}^{\mu\nu}$, Eq. (B8). Since the function $J_2(m, \Delta)$ does not enter our final results, we need only evaluate

$$\begin{aligned} \mathcal{J} \equiv (g_{\nu\mu} - v_\nu v_\mu) \mathcal{J}^{\mu\nu} &= \int \frac{d^4 q}{(2\pi)^4} \frac{i(g_{\nu\mu} - v_\nu v_\mu) q^\mu q^\nu}{(v \cdot q - \Delta + i\epsilon)(q^2 - m^2 + i\epsilon)} \\ &= \int \frac{d^4 q}{(2\pi)^4} \frac{-i\mathbf{q}^2}{(v \cdot q - \Delta + i\epsilon)(q^2 - m^2 + i\epsilon)} \\ &\rightarrow \frac{3\Delta}{(4\pi)^2} J_1(m, \Delta), \end{aligned} \quad (90)$$

where \mathbf{q} is the spatial 3-vector part of q^μ . In the last line, the arrow refers to the fact that the function J_1 arises after regularization and renormalization of the integral. A useful regulator in the present context is given by the insertion of a factor of $\exp(-\omega_q/\Lambda_0)$, where

Λ_0 is a cutoff. After performing the contour integral over q^0 ,

$$\begin{aligned}\mathcal{J} &= \int \frac{d^3q}{(2\pi)^3} \frac{\mathbf{q}^2}{2\omega_q(\omega_q + \Delta)} \\ &= \int \frac{d^3q}{(2\pi)^3} \frac{1}{2} - \int \frac{d^3q}{(2\pi)^3} \frac{\Delta}{2\omega_q} + \int \frac{d^3q}{(2\pi)^3} \frac{\Delta^2 - m^2}{2\omega_q(\omega_q + \Delta)} .\end{aligned}\quad (91)$$

The first term is a pure divergence with no m or Δ dependence. It is thus the same in finite volume or infinite volume [12]. The correction to the middle term is proportional to the correction to I_1 , since the same integral appears after performing the q^0 integration in Eq. (B5). Similarly, the integral in the third term is proportional to that arising from the q^0 integration in Eq. (B6), and the correction is therefore already known. We have

$$J_1(m, \Delta) \rightarrow J_1^{\text{fv}}(m, \Delta) = J_1(m, \Delta) + \delta J_1(m, \Delta, L) , \quad (92)$$

where

$$\delta J_1(m, \Delta, L) = \frac{m^2 - \Delta^2}{3\Delta^2} \delta I_2(m, \Delta, L) - \frac{m^2}{3} \delta_1(mL) \quad (93)$$

The correction to J_1^{sub} , Eq. (51), is

$$\delta J_1^{\text{sub}}(m, \Delta, L) = \delta J_1(m, \Delta, L) + \frac{16\pi^2 m^2}{3\Delta} J_{\text{FV}}(m, 0, L) , \quad (94)$$

where $J_{\text{FV}}(m, 0, L)$ is the same as Eq. (87) with $\mathcal{A} = 1$.

With the expressions in this section, it is straightforward to incorporate the corrections to I_1 , I_2 , and J_1 numerically into fits to finite-volume lattice data.

VI. CONCLUSIONS

We have presented the NLO expressions in partially quenched SXPT for the form factors associated with $B \rightarrow P_{xy}$ semileptonic decays, for both infinite and finite volume. Using a quark flow analysis, we have obtained these results by generalizing the NLO PQχPT expressions calculated in the continuum in Ref. [33]. The main subtlety in applying this technique is due to the appearance of taste matrices inside the Feynman diagrams, since non-trivial signs can arise from the anticommutation relations of the taste generators. We have shown that these signs can be accounted for by a careful analysis of the relevant quark flow diagrams.

The SXPT expressions are generally necessary for performing chiral fits to lattice simulations where staggered light quarks are used. For simpler quantities than the form factors,

SXPT has been seen to be essential [10, 20] in order to get reliable extrapolations both to the continuum limit and to the physical quark mass values. For form factors, the lattice data in Ref. [9] was not yet sufficiently precise for the SXPT expressions to be required (over continuum forms) for acceptable fits. However, we expect that the forms derived here will become more and more important as the lattice data improves.

Our results are valid to lowest order in HQET; in general, we neglect $1/m_B$ corrections. We do however include the B^*-B splitting Δ^* on internal B^* lines that are not in loops. This prescription allows the form factor f_p to have the physical m_B^* pole structure. Our treatment of the B^*-B splitting is similar, but not identical, to that of Refs. [33, 40]. Unlike those authors, we iterate self-energy contributions, namely Fig. 5(a) and the effect of the one-loop mass shift of the B , to all orders. This seems to us to be a natural choice, and also makes the one-loop corrections better behaved. Indeed, with the values of light quark masses and momenta typically used in staggered simulations [8, 9], the one-loop B mass shift can dominate other one-loop corrections, so summing such self-energy contributions to all orders seems entirely appropriate. The final answers are then expressed in terms of the splitting $\Delta_{yx}^* \equiv M_{B_y^*} - M_{B_x}$. In fitting lattice data, we suggest using the actual lattice values of this mass difference (at the simulated light quark mass values and lattice spacings), rather than applying a one-loop formula for the mass shifts.

Our primary results for the staggered, partially quenched case with three non-degenerate sea quarks are found in Sec. IV A. The form factor f_v (also known as f_{\parallel}) is given by Eq. (34) in terms of quantities defined in Eqs. (35), (52) and (53), as well as the wave function renormalization factors $\delta Z_{P_{xy}}$ and δZ_{B_x} that are listed in Eqs. (C1) and (C2) of Appendix C. Similarly, the form factor f_p (also known as f_{\perp}), is given by Eq. (36) in terms of quantities defined in Eqs. (31), (37), (38), and (54) through (57), as well as the wave function renormalization factors. We have also found a single relation, Eq. (40), among the parameters that control the analytic valence mass dependence. While this relation is also satisfied by the parameters written down in Ref. [33], it is important to know that it persists even in the presence of the complete NLO forms of the Lagrangian and current.

Appropriate limits of our expressions can be taken for various relevant cases, including the case of full (unquenched) staggered QCD (in Sec. IV B) and the case of continuum PQXPT with non-degenerate sea quark masses [Eqs. (63), (64), (C3), and (C4)]. Despite the fact that the latter are continuum results, they have not, to our knowledge, appeared

in the literature before. Finally, our expressions can be corrected for finite volume effects using the results of Sec. V.

ACKNOWLEDGMENTS

We thank J. Bailey, B. Grinstein, A. Kronfeld, P. Mackenzie, S. Sharpe and our colleagues in the MILC collaboration for helpful discussions. We also are grateful to D. Lin for discussions on finite volume corrections and for sharing with us the Mathematica code used to make the expansions in Ref. [42]. This work was partially supported by the U.S. Department of Energy under grant numbers DE-FG02-91ER40628 and DE-FG02-92ER40699.

APPENDIX A: FEYNMAN RULES

In this appendix we list the SXPT propagators and (some of) the vertices in Minkowski space [19], as well as the corresponding continuum versions.

In SXPT, the propagators for the heavy-light mesons are

$$\left\{ B_a B_b^\dagger \right\}(k) = \frac{i\delta_{ab}}{2(v \cdot k + i\epsilon)} , \quad (\text{A1})$$

$$\left\{ B_{\mu a}^* B_{\nu b}^{*\dagger} \right\}(k) = \frac{-i\delta_{ab}(g_{\mu\nu} - v_\mu v_\nu)}{2(v \cdot k - \Delta^* + i\epsilon)} . \quad (\text{A2})$$

Here a, b indicate the flavor-taste of the light quarks, and Δ^* is the B^*-B splitting in the chiral limit, which we often neglect since we work to leading order in HQET.

The $BB^*\pi$ vertex is:

$$\frac{g_\pi}{f} (B_a^\dagger B_{\mu b}^* - B_{\mu a}^{*\dagger} B_b) \partial^\mu \Phi_{ba} , \quad (\text{A3})$$

where repeated indices are summed. Other needed vertices come from the expansion of the LO current, Eq. (18). We have:

$$j_{\text{LO}}^{\mu,c} = \kappa B_a^{*\mu} \left(\delta_{ac} - \frac{1}{8f^2} \Phi_{ab} \Phi_{bc} + \dots \right) + \kappa v^\mu B_a \left(\frac{1}{2f} \Phi_{ac} + \dots \right) , \quad (\text{A4})$$

where repeated indices are again summed and \dots represents terms involving higher numbers of pions, as well as contributions from the axial vector part of the current, which are not relevant to the form factors.

If desired, each flavor-taste index can be replaced by a pair of indices representing flavor and taste separately. We use Latin indices in the middle of the alphabet (i, j, \dots) as pure

flavor indices, which take on the values $1, 2, \dots, N_{\text{sea}}$ in full QCD. Greek indices at the beginning of the alphabet ($\alpha, \beta, \gamma, \dots$) are used for quark taste indices, running from 1 to 4. Thus we can replace $a \rightarrow i\alpha$ and write, for example,

$$\left\{ B_{i\alpha} B_{j\beta}^\dagger \right\}(k) = \frac{i\delta_{ij}\delta_{\alpha\beta}}{2(v \cdot k + i\epsilon)}. \quad (\text{A5})$$

As in Refs. [13, 19], pion propagators are treated most easily by dividing them into connected and disconnected pieces, where the disconnected parts come from insertion (and iteration) of the hairpin vertices. The connected propagators are

$$\left\{ \Phi_{ij}^\Xi \Phi_{j'i'}^{\Xi'} \right\}_{\text{conn}}(p) = \frac{i\delta_{ii'}\delta_{jj'}\delta_{\Xi\Xi'}}{p^2 - m_{ij,\Xi}^2 + i\epsilon}, \quad (\text{A6})$$

where Ξ is one of the 16 meson tastes [as defined after Eq. (5)], and $m_{ij,\Xi}$ is the tree-level mass of a taste- Ξ meson composed of quarks of flavor i and j :

$$m_{ij,\Xi}^2 = \mu(m_i + m_j) + a^2\Delta_\Xi. \quad (\text{A7})$$

Here Δ_Ξ is the taste splitting, which can be expressed in terms of C_1 , C_3 , C_4 and C_6 in Eq. (16) [13]. There is a residual $SO(4)$ taste symmetry [11] at this order, implying that the mesons within a given taste multiplet (P , V , T , A , or I) are degenerate in mass. We therefore usually use the multiplet label to represent the splittings.

Since the heavy-light propagators are most simply written with flavor-taste indices, as in Eqs. (A1) and (A2), it is convenient to rewrite Eq. (A6) in flavor-taste notation also:

$$\left\{ \Phi_{ab} \Phi_{b'a'} \right\}_{\text{conn}}(p) \equiv \left\{ \Phi_{i\alpha,j\beta} \Phi_{j'\beta',i'\alpha'} \right\}_{\text{conn}}(p) = \sum_{\Xi} \frac{i\delta_{ii'}\delta_{jj'}T_{\alpha\beta}^\Xi T_{\beta'\alpha'}^\Xi}{p^2 - m_{ij,\Xi}^2 + i\epsilon}, \quad (\text{A8})$$

where T^Ξ are the 16 taste generators, Eq. (6).

For flavor-charged pions ($i \neq j$), the complete propagators are just the connected propagators in Eq. (A6) or (A8). However, for flavor-neutral pions ($i = j$), there are disconnected contributions coming from one or more hairpin insertions. At LO, these appear only for taste singlet, vector, or axial-vector pions. Denoting the Minkowski hairpin vertices as $-i\delta'_\Xi$, we have [13]:

$$\delta'_\Xi = \begin{cases} a^2\delta'_V, & T_\Xi \in \{\xi_\mu\} \text{ (taste vector);} \\ a^2\delta'_A, & T_\Xi \in \{\xi_{\mu 5}\} \text{ (taste axial-vector);} \\ 4m_0^2/3, & T_\Xi = \xi_I \text{ (taste singlet);} \\ 0, & T_\Xi \in \{\xi_{\mu\nu}, \xi_5\} \text{ (taste tensor or pseudoscalar)} \end{cases} \quad (\text{A9})$$

with

$$\delta'_{V(A)} \equiv \frac{16}{f^2}(C_{2V(A)} - C_{5V(A)}) . \quad (\text{A10})$$

The disconnected pion propagator is then

$$\left\{ \Phi_{ij}^\Xi \Phi_{j'i'}^{\Xi'} \right\}_{\text{disc}}(p) = \delta_{ij} \delta_{j'i'} \delta_{\Xi\Xi'} \mathcal{D}_{ii,i'i'}^\Xi , \quad (\text{A11})$$

where [13]

$$\mathcal{D}_{ii,i'i'}^\Xi = -i\delta'_\Xi \frac{i}{(p^2 - m_{ii,\Xi}^2)} \frac{i}{(p^2 - m_{i'i',\Xi}^2)} \frac{(p^2 - m_{U,\Xi}^2)(p^2 - m_{D,\Xi}^2)(p^2 - m_{S,\Xi}^2)}{(p^2 - m_{\pi^0,\Xi}^2)(p^2 - m_{\eta,\Xi}^2)(p^2 - m_{\eta',\Xi}^2)} . \quad (\text{A12})$$

For concreteness we have assumed that there are three sea-quark flavors: u , d , and s ; the generalization to N_{sea} flavors is immediate. Here $m_{U,\Xi} \equiv m_{uu,\Xi}$ is the mass of a taste- Ξ pion made from a u and a \bar{u} quark, neglecting hairpin mixing (and similarly for $m_{D,\Xi}$ and $m_{S,\Xi}$), $m_{\pi^0,\Xi}$, $m_{\eta,\Xi}$, and $m_{\eta',\Xi}$ are the mass eigenvalues after mixing is included, and the $i\epsilon$ terms have been left implicit. When specifying the particular member of a taste multiplet appearing in the disconnected propagator is unnecessary, we abuse this notation slightly following Eq. (A7) and refer to $\mathcal{D}_{ii,i'i'}^V$, $\mathcal{D}_{ii,i'i'}^A$, or $\mathcal{D}_{ii,i'i'}^I$. In flavor-taste notation we have:

$$\left\{ \Phi_{ab} \Phi_{b'a'} \right\}_{\text{disc}}(p) \equiv \left\{ \Phi_{i\alpha,j\beta} \Phi_{j'\beta',i'\alpha'} \right\}_{\text{disc}}(p) = \delta_{ij} \delta_{j'i'} \sum_{\Xi} T_{\alpha\beta}^\Xi T_{\beta'\alpha'}^\Xi \mathcal{D}_{ii,i'i'}^\Xi \quad (\text{A13})$$

For comparison, we now describe the continuum versions of the Feynman rules [18]. Since taste violations do not appear in \mathcal{L}_{HL} , Eq. (17), the continuum-theory version of Eqs. (A1) and (A2) are unchanged except that flavor-taste indices are replaced by pure flavor indices (i, j) :

$$\left\{ B_i B_j^\dagger \right\}(k) = \frac{i\delta_{ij}}{2(v \cdot k + i\epsilon)} \quad [\text{continuum}], \quad (\text{A14})$$

$$\left\{ B_{\mu i}^* B_{\nu j}^{*\dagger} \right\}(k) = \frac{-i\delta_{ij}(g_{\mu\nu} - v_\mu v_\nu)}{2(v \cdot k + i\epsilon)} \quad [\text{continuum}]. \quad (\text{A15})$$

Similarly, the continuum $BB^*\pi$ [18] and current vertices are identical to those in SXPT, aside from the redefinition of the indices and a factor of 2 for each Φ_{ab} field due to the non-standard normalization of the generators in the SXPT case, Eq. (6). The continuum version of Eq. (A3) is

$$2\frac{ig_\pi}{f} \left(B_{\mu i}^{*\dagger} B_j - B_i^\dagger B_{\mu j}^* \right) \partial^\mu \Phi_{ji} \quad [\text{continuum}]; \quad (\text{A16})$$

while the continuum version of Eq. (A4) is

$$j_{\text{LO}}^{\mu,k} = \kappa B_\ell^{*\mu} \left(\delta_{\ell k} - \frac{1}{2f^2} \Phi_{\ell i} \Phi_{ik} + \dots \right) + \kappa v^\mu B_\ell \left(\frac{1}{f} \Phi_{\ell k} + \dots \right) \quad [\text{continuum}]. \quad (\text{A17})$$

Because of taste-violations in the SXPT pion sector, the differences between the propagators Eqs. (A6), (A11) and (A12) and their continuum versions are slightly less trivial. The continuum connected propagator is

$$\left\{ \Phi_{ij} \Phi_{j'i'} \right\}_{\text{conn}}(p) = \frac{i \delta_{ii'} \delta_{jj'}}{p^2 - m_{ij}^2 + i\epsilon} \quad [\text{continuum}], \quad (\text{A18})$$

with

$$m_{ij}^2 = \mu(m_i + m_j) \quad [\text{continuum}]. \quad (\text{A19})$$

The continuum disconnected propagator is

$$\left\{ \Phi_{ij} \Phi_{j'i'} \right\}_{\text{disc}}(p) = \delta_{ij} \delta_{j'i'} \mathcal{D}_{ii,i'i'} \quad [\text{continuum}], \quad (\text{A20})$$

where [13]

$$\mathcal{D}_{ii,i'i'} = -i\delta' \frac{i}{(p^2 - m_{ii}^2)} \frac{i}{(p^2 - m_{i'i'}^2)} \frac{(p^2 - m_U^2)(p^2 - m_D^2)(p^2 - m_S^2)}{(p^2 - m_{\pi^0}^2)(p^2 - m_\eta^2)(p^2 - m_{\eta'}^2)} \quad [\text{continuum}], \quad (\text{A21})$$

with now $\delta' = m_0^2/3$.

Note the difference in normalization between δ' and the SXPT taste-singlet hairpin, δ'_I , Eq. (A9). This arises from the fact that $m_0^2/3$ is defined to be the strength of the hairpin vertex when one has a single species of quark on each side of the vertex [12]. In the staggered case, each normalized taste-singlet field is made out of four species (tastes), for example $\phi^I = \frac{1}{2}(\phi_{11} + \phi_{22} + \phi_{33} + \phi_{44})$, where ϕ is flavor neutral, and only taste indices are shown. In the disconnected propagator of two such fields, there are 16 terms, and a factor of $(1/2)^2$ from the normalization, so there is an overall factor of 4 relative to a single-species disconnected propagator, such as that of ϕ_{11} with ϕ_{22} . At one loop, the “external” fields in this propagator are always valence fields, so the normalization issue has nothing directly to do with the fourth root trick for staggered sea quarks. (The normalization is in fact compensated by the extra factors of 2 in the continuum vertices.) The rooting does however affect the η'_I mass that appears in denominator of Eq. (A21), which comes from iterations of the hairpin and therefore involves sea quarks. The end result is that $m_{\eta',I}^2 \approx N_{\text{sea}} m_0^2/3$ (for large m_0), rather than $\approx 4N_{\text{sea}} m_0^2/3$, the value in the unrooted theory [13]. In the continuum, we also have $m_{\eta'}^2 \approx N_{\text{sea}} m_0^2/3$.

APPENDIX B: INTEGRALS

Here we collect the integrals needed in evaluating the diagrams for the semileptonic form factors [19, 33].

The disconnected propagators can be written as a sum of single or double poles using the (Euclidean) residue functions introduced in Ref. [13] or their Minkowski-space versions. We define $\{m\} \equiv \{m_1, m_2, \dots, m_n\}$ as the set of masses that appear in the denominator of Eq. (A12), and $\{\mu\} \equiv \{\mu_1, \mu_2, \dots, \mu_k\}$ as the numerator set of masses. Then, for $n > k$ and all masses distinct, we have:

$$\mathcal{I}^{[n,k]}(\{m\};\{\mu\}) \equiv \frac{\prod_{i=1}^k (q^2 - \mu_i^2)}{\prod_{j=1}^n (q^2 - m_j^2 + i\epsilon)} = \sum_{j=1}^n \frac{\hat{R}_j^{[n,k]}(\{m\};\{\mu\})}{q^2 - m_j^2 + i\epsilon}, \quad (\text{B1})$$

where the Minkowski space residues $\hat{R}_j^{[n,k]}$ are given by

$$\hat{R}_j^{[n,k]}(\{m\};\{\mu\}) \equiv \frac{\prod_{i=1}^k (m_j^2 - \mu_i^2)}{\prod_{r \neq j} (m_j^2 - m_r^2)}. \quad (\text{B2})$$

If there is one double pole term for $q^2 = m_\ell^2$ (where $m_\ell \in \{m\}$), then

$$\begin{aligned} \mathcal{I}_{\text{dp}}^{[n,k]}(m_\ell; \{m\}; \{\mu\}) &\equiv \frac{\prod_{i=1}^k (q^2 - \mu_i^2)}{(q^2 - m_\ell^2 + i\epsilon) \prod_{j=1}^n (q^2 - m_j^2 + i\epsilon)} \\ &= \frac{\partial}{\partial m_\ell^2} \sum_{j=1}^n \frac{\hat{R}_j^{[n,k]}(\{m\};\{\mu\})}{q^2 - m_j^2 + i\epsilon}. \end{aligned} \quad (\text{B3})$$

In the end we want to write the results in terms of the Euclidean-space residues $R_j^{[n,k]}$, because they are ones we have used previously [13, 19]. In Euclidean space the sign of each factor in Eq. (B2) is changed. We therefore have

$$R_j^{[n,k]}(\{m\};\{\mu\}) \equiv \frac{\prod_{i=1}^k (\mu_i^2 - m_j^2)}{\prod_{r \neq j} (m_r^2 - m_j^2)} = (-1)^{n+k-1} \hat{R}_j^{[n,k]}(\{m\};\{\mu\}). \quad (\text{B4})$$

The integrals needed for the form factors are ([17, 33])

$$\mathcal{I}_1 = \mu^{4-d} \int \frac{d^d q}{(2\pi)^d} \frac{i}{q^2 - m^2 + i\epsilon} \rightarrow \frac{1}{(4\pi)^2} I_1(m), \quad (\text{B5})$$

$$\mathcal{I}_2 = \mu^{4-d} \int \frac{d^d q}{(2\pi)^d} \frac{i}{(v \cdot q - \Delta + i\epsilon)(q^2 - m^2 + i\epsilon)} \rightarrow \frac{1}{(4\pi)^2} \frac{1}{\Delta} I_2(m, \Delta), \quad (\text{B6})$$

$$\mathcal{I}_3^\mu = \mu^{4-d} \int \frac{d^d q}{(2\pi)^d} \frac{i q^\mu}{(v \cdot q - \Delta + i\epsilon)(q^2 - m^2 + i\epsilon)} \rightarrow \frac{v^\mu}{(4\pi)^2} [I_2(m, \Delta) + I_1(m)], \quad (\text{B7})$$

$$\mathcal{J}^{\mu\nu} = \mu^{4-d} \int \frac{d^d q}{(2\pi)^d} \frac{i q^\mu q^\nu}{(v \cdot q - \Delta + i\epsilon)(q^2 - m^2 + i\epsilon)} \rightarrow \frac{\Delta}{(4\pi)^2} [J_1(m, \Delta) g^{\mu\nu} + J_2(m, \Delta) v^\mu v^\nu], \quad (\text{B8})$$

where the arrows represent the fact that the r.h.s. of these expressions have already been renormalized (unlike the corresponding equations in Ref. [33]).

APPENDIX C: WAVEFUNCTION RENORMALIZATION FACTORS

The one loop chiral corrections to the wave function renormalization factors Z_B and Z_P are [13, 19]

$$\begin{aligned}
\delta Z_{P_{xy}} = & \frac{1}{3(4\pi f)^2} \left\{ \frac{1}{16} \sum_{f,\Xi} [I_1(m_{xf,\Xi}) + I_1(m_{yf,\Xi})] \right. \\
& + \frac{1}{3} \left[\sum_{j \in \mathcal{M}^{(3,x)}} \frac{\partial}{\partial m_{X,I}^2} \left(R_j^{[3,3]} \left(\mathcal{M}_I^{(3,x)}; \mu_I^{(3)} \right) I_1(m_{j,I}) \right) \right. \\
& + \sum_{j \in \mathcal{M}^{(3,y)}} \frac{\partial}{\partial m_{Y,I}^2} \left(R_j^{[3,3]} \left(\mathcal{M}_I^{(3,y)}; \mu_I^{(3)} \right) I_1(m_{j,I}) \right) \\
& + 2 \sum_{j \in \mathcal{M}^{(4,xy)}} R_j^{[4,3]} \left(\mathcal{M}_I^{(4,xy)}; \mu_I^{(3)} \right) I_1(m_{j,I}) \left. \right] \\
& + a^2 \delta'_V \left[\sum_{j \in \mathcal{M}^{(4,x)}} \frac{\partial}{\partial m_{X,V}^2} \left(R_j^{[4,3]} \left(\mathcal{M}_V^{(4,x)}; \mu_V^{(3)} \right) I_1(m_{j,V}) \right) \right. \\
& + \sum_{j \in \mathcal{M}^{(4,y)}} \frac{\partial}{\partial m_{Y,V}^2} \left(R_j^{[4,3]} \left(\mathcal{M}_V^{(4,y)}; \mu_V^{(3)} \right) I_1(m_{j,V}) \right) \\
& - 2 \sum_{j \in \mathcal{M}^{(5,xy)}} R_j^{[5,3]} \left(\mathcal{M}_V^{(5,xy)}; \mu_V^{(3)} \right) I_1(m_{j,V}) \left. \right] \\
& \left. + [V \rightarrow A] \right\}, \tag{C1}
\end{aligned}$$

$$\begin{aligned}
\delta Z_{B_x} = & \frac{-3g_\pi^2}{(4\pi f)^2} \left\{ \frac{1}{16} \sum_{f,\Xi} I_1(m_{xf,\Xi}) \right. \\
& + \frac{1}{3} \sum_{j \in \mathcal{M}^{(3,x)}} \frac{\partial}{\partial m_{X,I}^2} \left[R_j^{[3,3]} \left(\mathcal{M}_I^{(3,x)}; \mu_I^{(3)} \right) I_1(m_{j,I}) \right] \\
& + a^2 \delta'_V \sum_{j \in \mathcal{M}^{(4,x)}} \frac{\partial}{\partial m_{X,V}^2} \left[R_j^{[4,3]} \left(\mathcal{M}_V^{(4,x)}; \mu_V^{(3)} \right) I_1(m_{j,V}) \right] + [V \rightarrow A] \left. \right\}, \tag{C2}
\end{aligned}$$

where f runs over the sea quarks (u, d, s).

For the continuum result in partially quenched χ Pt, we can simply set $a = 0$ and ignore taste splittings. In the 1+1+1 case, we get

$$\begin{aligned} \delta Z_{P_{xy}}^{\text{cont}} = & \frac{1}{3(4\pi f)^2} \left\{ \sum_f [I_1(m_{xf}) + I_1(m_{yf})] \right. \\ & + \frac{1}{3} \left[\sum_{j \in \mathcal{M}^{(3,x)}} \frac{\partial}{\partial m_X^2} \left(R_j^{[3,3]}(\mathcal{M}^{(3,x)}; \mu^{(3)}) I_1(m_j) \right) \right. \\ & + \sum_{j \in \mathcal{M}^{(3,y)}} \frac{\partial}{\partial m_Y^2} \left(R_j^{[3,3]}(\mathcal{M}^{(3,y)}; \mu^{(3)}) I_1(m_j) \right) \\ & \left. \left. + 2 \sum_{j \in \mathcal{M}^{(4,xy)}} R_j^{[4,3]}(\mathcal{M}^{(4,xy)}; \mu^{(3)}) I_1(m_j) \right] \right\}, \end{aligned} \quad (\text{C3})$$

$$\begin{aligned} \delta Z_{B_x}^{\text{cont}} = & \frac{-3g_\pi^2}{(4\pi f)^2} \left\{ \sum_f I_1(m_{xf}) \right. \\ & \left. + \frac{1}{3} \sum_{j \in \mathcal{M}^{(3,x)}} \frac{\partial}{\partial m_X^2} \left[R_j^{[3,3]}(\mathcal{M}^{(3,x)}; \mu^{(3)}) I_1(m_j) \right] \right\} \end{aligned} \quad (\text{C4})$$

Returning to $a \neq 0$, and taking the valence quark masses to be $m_x = m_y = m_u = m_d$, we have the 2+1 full QCD pion result in S χ PT:

$$\begin{aligned} \delta Z_\pi = & \frac{1}{3(4\pi f)^2} \left\{ \frac{1}{16} \sum_{\Xi} [4I_1(m_{\pi,\Xi}) + 2I_1(m_{K,\Xi})] \right. \\ & + (-4a^2 \delta'_V) \left[\frac{(m_{S_V}^2 - m_{\pi_V}^2)}{(m_{\eta_V}^2 - m_{\pi_V}^2)(m_{\eta'_V}^2 - m_{\pi_V}^2)} I_1(m_{\pi_V}) + \frac{(m_{S_V}^2 - m_{\eta_V}^2)}{(m_{\pi_V}^2 - m_{\eta_V}^2)(m_{\eta'_V}^2 - m_{\eta_V}^2)} I_1(m_{\eta_V}) \right. \\ & \left. \left. + \frac{(m_{S_V}^2 - m_{\eta'_V}^2)}{(m_{\pi_V}^2 - m_{\eta'_V}^2)(m_{\eta_V}^2 - m_{\eta'_V}^2)} I_1(m_{\eta'_V}) \right] + [V \rightarrow A] \right\}. \end{aligned} \quad (\text{C5})$$

Taking the valence quark masses to be $m_x = m_u = m_d$ and $m_y = m_s$ gives the 2+1 full

QCD kaon result:

$$\begin{aligned}
\delta Z_K = & \frac{1}{3(4\pi f)^2} \left\{ \frac{1}{16} \sum_{\Xi} (2I_1(m_{\pi,\Xi}) + 3I_1(m_{K,\Xi}) + I_1(m_{S,\Xi})) \right. \\
& - \frac{1}{2} I_1(m_{\pi_I}) + \frac{3}{2} I_1(m_{\eta_I}) - I_1(m_{S_I}) \\
& + (-a^2 \delta'_V) \left(\frac{(m_{S_V}^2 + m_{\pi_V}^2 - 2m_{\eta_V}^2)^2}{(m_{\pi_V}^2 - m_{\eta_V}^2)(m_{S_V}^2 - m_{\eta_V}^2)(m_{\eta'_V}^2 - m_{\eta_V}^2)} I_1(m_{\eta_V}) \right. \\
& + \frac{(m_{S_V}^2 + m_{\pi_V}^2 - 2m_{\eta'_V}^2)^2}{(m_{\pi_V}^2 - m_{\eta'_V}^2)(m_{S_V}^2 - m_{\eta'_V}^2)(m_{\eta_V}^2 - m_{\eta'_V}^2)} I_1(m_{\eta'_V}) \\
& + \frac{m_{S_V}^2 - m_{\pi_V}^2}{(m_{\eta_V}^2 - m_{\pi_V}^2)(m_{\eta'_V}^2 - m_{\pi_V}^2)} I_1(m_{\pi_V}) + \frac{m_{\pi_V}^2 - m_{S_V}^2}{(m_{\eta_V}^2 - m_{S_V}^2)(m_{\eta'_V}^2 - m_{S_V}^2)} I_1(m_{S_V}) \Big) \\
& \left. + (V \rightarrow A) \right\}. \tag{C6}
\end{aligned}$$

Setting $m_x = m_u = m_d$ in Eq. (C2) results in the 2+1 full QCD result for the B wavefunction renormalization:

$$\begin{aligned}
\delta Z_B = & \frac{3g_\pi^2}{(4\pi f)^2} \left\{ -\frac{1}{16} \sum_{\Xi} [2I_1(m_{\pi,\Xi}) + I_1(m_{K,\Xi})] + \frac{1}{2} I_1(m_{\pi_I}) - \frac{1}{6} I_1(m_{\eta_I}) \right. \\
& + a^2 \delta'_V \left[\frac{(m_{S_V}^2 - m_{\pi_V}^2)}{(m_{\eta_V}^2 - m_{\pi_V}^2)(m_{\eta'_V}^2 - m_{\pi_V}^2)} I_1(m_{\pi_V}) + \frac{(m_{S_V}^2 - m_{\eta_V}^2)}{(m_{\pi_V}^2 - m_{\eta_V}^2)(m_{\eta'_V}^2 - m_{\eta_V}^2)} I_1(m_{\eta_V}) \right. \\
& \left. + \frac{(m_{S_V}^2 - m_{\eta'_V}^2)}{(m_{\pi_V}^2 - m_{\eta'_V}^2)(m_{\eta_V}^2 - m_{\eta'_V}^2)} I_1(m_{\eta'_V}) \right] + [V \rightarrow A] \Big\}. \tag{C7}
\end{aligned}$$

Finally, putting $m_x = m_s$ and $m_u = m_d$ in Eq. (C2), we obtain the full QCD B_s renormalization factor in the 2+1 case:

$$\begin{aligned}
\delta Z_{B_s} = & \frac{3g_\pi^2}{(4\pi f)^2} \left\{ -\frac{1}{16} \sum_{\Xi} [I_1(m_{S,\Xi}) + 2I_1(m_{K,\Xi})] + I_1(m_{S_I}) - \frac{2}{3} I_1(m_{\eta_I}) \right. \\
& + (-a^2 \delta'_V) \left[\frac{(m_{S_V}^2 - m_{\pi_V}^2)}{(m_{S_V}^2 - m_{\eta_V}^2)(m_{S_V}^2 - m_{\eta'_V}^2)} I_1(m_{S_V}) + \frac{(m_{\eta_V}^2 - m_{\pi_V}^2)}{(m_{\eta_V}^2 - m_{S_V}^2)(m_{\eta_V}^2 - m_{\eta'_V}^2)} I_1(m_{\eta_V}) \right. \\
& \left. + \frac{(m_{\eta'_V}^2 - m_{\pi_V}^2)}{(m_{\eta'_V}^2 - m_{S_V}^2)(m_{\eta'_V}^2 - m_{\eta_V}^2)} I_1(m_{\eta'_V}) \right] + [V \rightarrow A] \Big\}. \tag{C8}
\end{aligned}$$

[1] T. Onogi, PoS **LAT2006**, 017 (2006) [arXiv:hep-lat/0610115].

[2] M. Okamoto, PoS **LAT2005**, 013 (2006) [arXiv:hep-lat/0510113].

- [3] M. Wingate, Nucl. Phys. Proc. Suppl. **140**, 68 (2005) [arXiv:hep-lat/0410008].
- [4] A. S. Kronfeld, Nucl. Phys. Proc. Suppl. **129**, 46 (2004) [arXiv:hep-lat/0310063].
- [5] M. Wingate, *et al.*, Phys. Rev. D **67**, 054505 (2003) [arXiv:hep-lat/0211014].
- [6] M. Wingate, C. Davies, A. Gray, E. Gulez, G. P. Lepage and J. Shigemitsu, Nucl. Phys. Proc. Suppl. **129**, 325 (2004) [arXiv:hep-lat/0309092].
- [7] M. Wingate, C. T. H. Davies, A. Gray, G. P. Lepage and J. Shigemitsu, Phys. Rev. Lett. **92**, 162001 (2004) [arXiv:hep-ph/0311130].
- [8] E. Gulez *et al.*, Phys. Rev. D **73**, 074502 (2006) [arXiv:hep-lat/0601021]; J. Shigemitsu *et al.*, Nucl. Phys. Proc. Suppl. **129**, 331 (2004) [arXiv:hep-lat/0309039].
- [9] C. Aubin *et al.* [Fermilab Lattice, MILC, and HPQCD Collaborations], Phys. Rev. Lett. **94**, 011601 (2005) [arXiv:hep-ph/0408306]; M. Okamoto *et al.* [Fermilab Lattice, MILC and HPQCD Collaborations], Nucl. Phys. Proc. Suppl. **140**, 461 (2005) [arXiv:hep-lat/0409116]; P. B. Mackenzie *et al.* [Fermilab Lattice, MILC and HPQCD Collaborations], PoS **LAT2005**, 207 (2006).
- [10] C. Aubin *et al.* [Fermilab Lattice, MILC, and HPQCD Collaborations], Phys. Rev. Lett. **95**, 122002 (2005) [arXiv:hep-lat/0506030].
- [11] W. Lee and S. Sharpe Phys. Rev. **D60**, 114503 (1999) [arXiv: hep-lat/9905023].
- [12] C. Bernard, Phys. Rev. **D65**, 054031 (2001) [arXiv: hep-lat/0111051].
- [13] C. Aubin and C. Bernard, Phys. Rev. D **68**, 034014 (2003) [arXiv:hep-lat/0304014]; Phys. Rev. D **68**, 074011 (2003) [arXiv:hep-lat/0306026]; Nucl. Phys. **B** (Proc. Suppl.) **129-130C** (2004), 182 [arXiv:hep-lat/0308036].
- [14] G. Burdman and J. F. Donoghue, Phys. Lett. B **280**, 287 (1992); M. B. Wise, Phys. Rev. D **45**, 2188 (1992); T. M. Yan *et al.*, Phys. Rev. D **46**, 1148 (1992) [Erratum-ibid. D **55**, 5851 (1997)].
- [15] B. Grinstein, *et al.*, Nucl. Phys. B **380**, 369 (1992) [arXiv:hep-ph/9204207].
- [16] J. L. Goity, Phys. Rev. D **46**, 3929 (1992) [arXiv:hep-ph/9206230].
- [17] C. G. Boyd and B. Grinstein, Nucl. Phys. B **442**, 205 (1995) [arXiv:hep-ph/9402340].
- [18] A. Manohar and M. Wise, *Heavy Quark Physics*, Cambridge University Press (2000) and references therein.
- [19] C. Aubin and C. Bernard, Phys. Rev. D **73**, 014515 (2006) [arXiv:hep-lat/0510088].
- [20] C. Aubin *et al.* [MILC Collaboration], Phys. Rev. D **70**, 114501 (2004) [arXiv:hep-lat/0407028]

- and Phys. Rev. D **70**, 094505 (2004) [arXiv:hep-lat/0402030].
- [21] E. Marinari, G. Parisi and C. Rebbi, Nucl. Phys. B **190**, 734 (1981).
 - [22] C. Bernard, M. Golterman and Y. Shamir, Phys. Rev. D **73**, 114511 (2006) [arXiv:hep-lat/0604017].
 - [23] Y. Shamir, Phys. Rev. D **75**, 054503 (2007) [arXiv:hep-lat/0607007].
 - [24] C. Bernard, Phys. Rev. D **73**, 114503 (2006) [arXiv:hep-lat/0603011].
 - [25] S. Sharpe, Proceedings of Science (Lattice 2006) 022 (2006) [arXiv:he-lat/0610094].
 - [26] C. Bernard, M. Golterman, and Y. Shamir, Proceedings of Science (Lattice 2006) 205 (2006) [arXiv:hep-lat/0610003].
 - [27] S. Dürer and C. Hoelbling, Phys. Rev. D **69**, 034503 (2004) [arXiv:hep-lat/0311002], Phys. Rev. D **71**, 054501 (2005) [arXiv:hep-lat/0411022] and Phys. Rev. D **74**, 014513 (2006) [arXiv:hep-lat/0604005]; D. H. Adams, Phys. Rev. Lett. **92**, 162002 (2004) [arXiv:hep-lat/0312025] and Phys. Rev. D **72**, 114512 (2005) [arXiv:hep-lat/0411030]; E. Foliana, A. Hart and C. T. H. Davies, Phys. Rev. Lett. **93**, 241601 (2004) [arXiv:hep-lat/0406010]; S. Dürer, C. Hoelbling and U. Wenger, Phys. Rev. D **70**, 094502 (2004) [arXiv:hep-lat/0406027]; F. Maresca and M. Peardon, arXiv:hep-lat/0411029; Y. Shamir, Phys. Rev. D **71**, 034509 (2005) [arXiv:hep-lat/0412014]; C. Bernard *et al.* [MILC Collaboration], PoS **LAT2005**, 114 [arXiv:hep-lat/0509176]; A. Hasenfratz and R. Hoffmann, Phys. Rev. D **74**, 014511 (2006) [arXiv:hep-lat/0604010].
 - [28] J. Laiho, Proceedings of Science, PoS(LAT2005)221, arXiv:hep-lat/0510058; J. Laiho and R. S. Van de Water, Phys. Rev. D **73**, 054501 (2006) [arXiv:hep-lat/0512007].
 - [29] S. R. Sharpe, Phys. Rev. D **46**, 3146 (1992) [arXiv:hep-lat/9205020].
 - [30] P. H. Damgaard and K. Splittorff, Phys. Rev. D **62**, 054509 (2000) [arXiv:hep-lat/0003017]; C. Aubin and C. Bernard, Nucl. Phys. **B** (Proc. Suppl.) **129-130** (2004), 182 [arXiv:hep-lat/0308036].
 - [31] A. S. Kronfeld, Phys. Rev. D **62**, 014505 (2000) [arXiv:hep-lat/0002008].
 - [32] C. Bernard *et al.* [MILC Collaboration], PoS **LAT2006** (2006) 163 [arXiv:hep-lat/0609053].
 - [33] D. Bećirević, S. Prelovsek and J. Zupan, Phys. Rev. D **68**, 074003 (2003) [arXiv:hep-lat/0305001].
 - [34] C. Aubin and C. Bernard, Nucl. Phys. **B** (Proc. Suppl.) **140** (2005), 491 [arXiv:hep-lat/0409027].

- [35] S. R. Sharpe, Phys. Rev. D **56**, 7052 (1997) [Erratum-ibid. D **62**, 099901 (2000)]
[arXiv:hep-lat/9707018].
- [36] S. R. Sharpe and Y. Zhang, Phys. Rev. D **53**, 5125 (1996) [arXiv:hep-lat/9510037].
- [37] S. Sharpe and N. Shoresh, Phys. Rev. **D64**, 114510 (2001) [arXiv:hep-lat/0108003].
- [38] J. Gasser and H. Leutwyler, Nucl. Phys. **B250**, 465, 1985.
- [39] S. R. Sharpe and R. S. Van de Water, Phys. Rev. D **71**, 114505 (2005) [arXiv:hep-lat/0409018].
- [40] A. F. Falk and B. Grinstein, Nucl. Phys. B **416**, 771 (1994) [arXiv:hep-ph/9306310].
- [41] I. W. Stewart, Nucl. Phys. B **529**, 62 (1998) [arXiv:hep-ph/9803227].
- [42] D. Arndt and C. J. D. Lin, Phys. Rev. D **70**, 014503 (2004) [arXiv:hep-lat/0403012].

TABLE I: Connecting the one-loop diagrams from Ref. [33] (left column) and this paper (right column).

Ref. [33]	This work
(4)	Fig. 4(a)
(7)	Fig. 5(a)
(9)	Fig. 5(b)
(12)	Fig. 5(c)
(13)	Fig. 5(d)
(14)	Fig. 4(b)

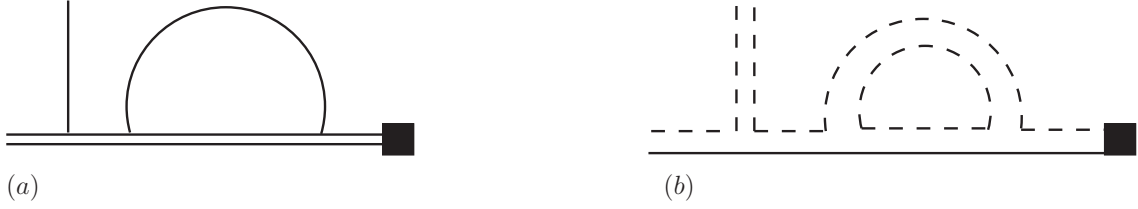


FIG. 1: Example of a connected one-loop form factor diagram at (a) the meson level and (b) the quark level. For the meson diagram, the double line is a heavy-light meson while the single line is a pion. For the quark-level diagram, the solid line is a heavy quark and the dashed line is a light quark. The internal sea quark loop is required by the (quark-flow) connected pion propagator; purely valence diagrams are only possible with a disconnected pion propagator. Therefore this diagram gives rise to a factor of N_{sea} in the degenerate case.

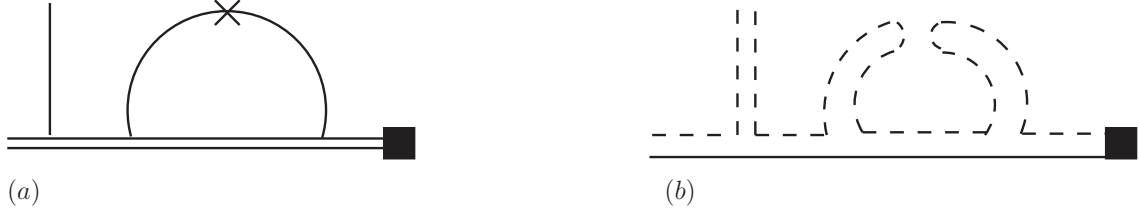


FIG. 2: Example of a disconnected one-loop form factor diagram at (a) the meson level and (b) the quark level. The cross in the meson diagram represents the two-point interactions in χ PT, and is represented by the “hairpin” in the quark-level diagram. There are no factors of N_{sea} but instead factors of $1/N_{\text{sea}}$ coming from the decoupling of the η' .

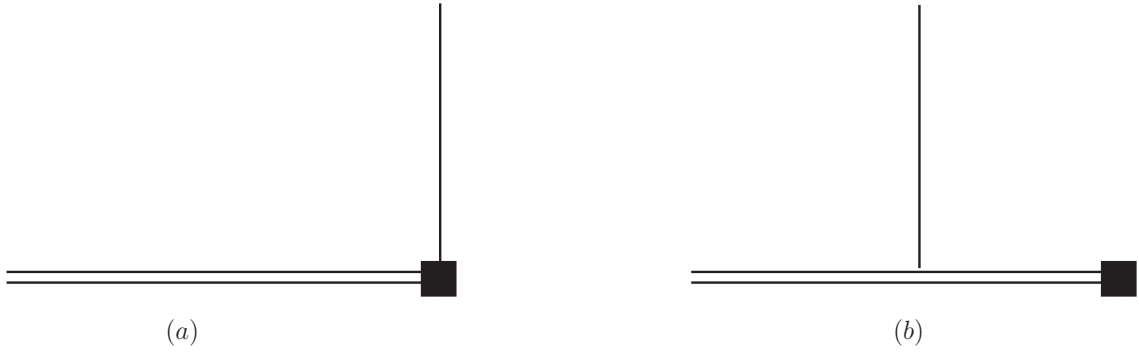


FIG. 3: Tree level diagrams for (a) f_v and (b) f_p . The double line is the heavy-light meson and the single line is the pion.

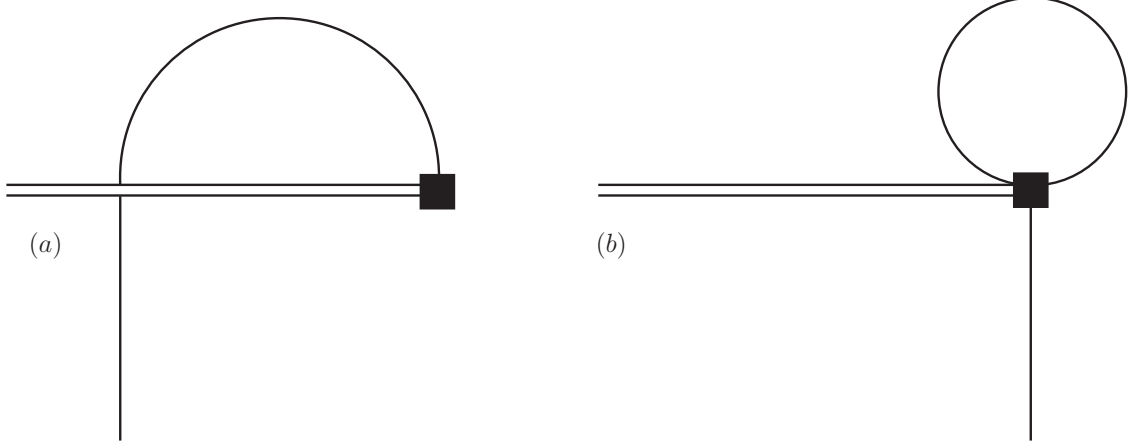


FIG. 4: One-loop f_v diagrams. The internal light meson lines may in general be connected or disconnected: possible hairpin insertions are not shown explicitly.

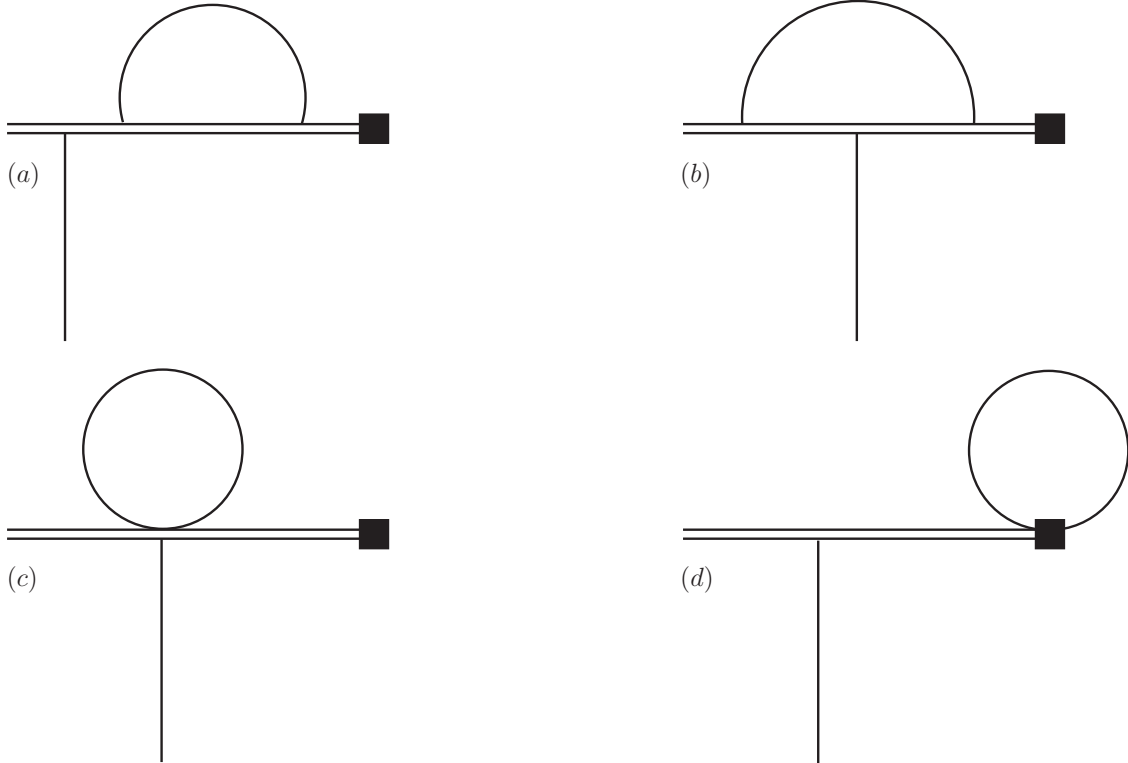


FIG. 5: One-loop f_p diagrams. The internal light meson lines may in general be connected or disconnected: possible hairpin insertions are not shown explicitly.

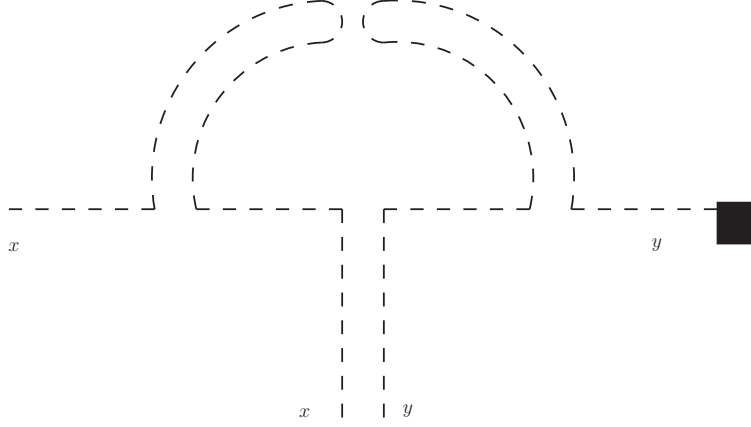


FIG. 6: The quark-flow diagram for Fig. 5(b), omitting the heavy quark line for clarity. The mesons in the loop are X and Y mesons, flavor-neutral mesons made up of x and y quarks. Note that even though only a single hairpin insertion is shown explicitly, the figure should be interpreted as representing all diagrams with one or more hairpins.

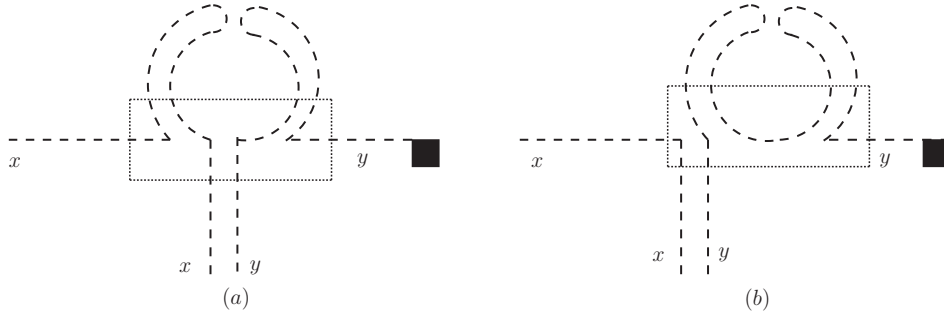


FIG. 7: Possible quark-flow diagrams for Fig. 5(c) with a disconnected meson propagator in the loop. The solid rectangle encloses the 5-point vertex of Fig. 5(c). The heavy quark line has been omitted for clarity. A “reflected” version of diagram (b), with the outgoing pion on the other side of the vertex, is also possible.

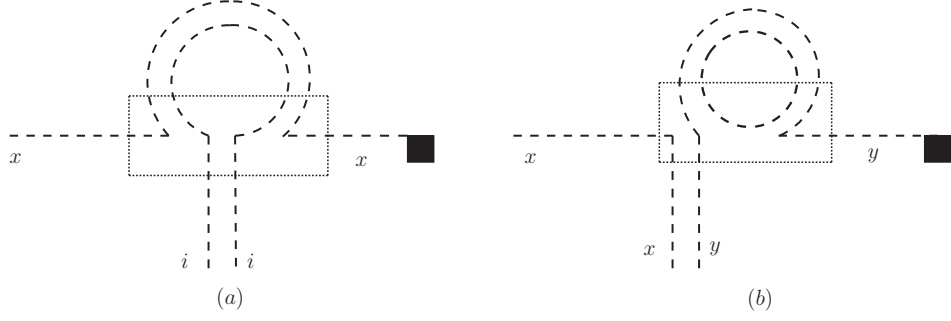


FIG. 8: Possible quark-flow diagrams for Fig. 5(c) with a connected meson propagator in the loop. The solid rectangle encloses the 5-point vertex of Fig. 5(c). The heavy quark line has been omitted for clarity. Since we have assumed that x and y are different flavors, diagram (a) cannot occur in our case. Diagram (b) can occur, as can a “reflected” version with the outgoing pion on the other side of the vertex.